Exhumation and deformation history of the lower crustal section of the Valstrona di Omegna in the Ivrea Zone, southern Alps

S. Siegesmund, P. Layer, I. Dunkl, A. Vollbrecht, A. Steenken, K. Wemmer and H. Ahrendt

Geological Society, London, Special Publications 2008; v. 298; p. 45-68
doi:10.1144/SP298.3

Exhumation and deformation history of the lower crustal section of the Valstrona di Omegna in the Ivrea Zone, southern Alps

S. SIEGESMUND[1], P. LAYER[2], I. DUNKL[1], A. VOLLBRECHT[1], A. STEENKEN[3], K. WEMMER[1] & H. AHRENDT[1,†]

[1]*Gottinger Zentrum Geowissenschaften, University of Göttingen, Goldschmidtstrasse 03, D–37077, Göttingen (e-mail: ssieges@gwdg.de)*

[2]*Geophysical Institute, University of Alaska Fairbanks, Fairbanks, Alaska 99775, USA*

[3]*Instituto de Geociências, Universidade de São Paulo, Rua do Lago 562, Cidade Universitária, 05508-080 - São Paulo, SP-Brazil*

Abstract: The Ivrea Zone (southern Alps) is one of the key regions interpreted as exposing a section of the lower continental crust and was the subject of several review-type articles. The Ivrea–Verbano Zone was rotated into an upright position along the Insubric mylonite belt. In the southeast, this unit is in contact with the Strona Ceneri Zone, which is interpreted as upper continental crust crossing the Permian Cossato–Mergozzo–Brissagio Line (CMB Line). The CMB mylonites are locally overprinted by the mylonites and cataclasites of the Pogallo Line, which was active during the Jurassic. In addition, the sinistral, steeply inclined Rosarolo shear zone was active over a long time span from the ductile into the brittle field, i.e. from the Early Permian (high-temperature ultra-mylonites) to the Neo-Alpine basic dykes and pseudotachylites. The high-temperature mylonites accommodated crustal extension and may be related to normal faults generated by magmatic underplating. The reactivation at different crustal levels during exhumation and tilting is documented by strain increments at decreasing P/T conditions. Its present subvertical orientation was attained during the Neo-Alpine deformation. Constraints on its exhumation history are based on new $^{40}Ar/^{39}Ar$ hornblende ages, K–Ar biotite ages and zircon fission-track data along the NE–SW trending Valstrona section. A re-interpretation of existing U–Pb monazite ages is included, based on a higher closure temperature for monazite. The oldest monazite ages are observed in proximity to the Pogallo Line (*c*. 292 Ma). Heat input by mafic intrusions was sufficient to reset the U–Pb monazite system, as is evidenced by the youngest ages in the vicinity of the Insubric Line. The re-interpretation favours the hypothesis that the oldest monazite ages are the result of complete resetting by a Permian thermal event. The $^{40}Ar/^{39}Ar$ hornblende ages and K–Ar biotite ages document the cooling after Permian heating. Roughly parallel age progressions decrease from the Pogallo Line (hornblende: 271 Ma vs. biotite: 227 Ma) towards the Insubric Line (hornblende: 201 Ma vs. biotite: 156 Ma). Zircon fission-track ages run parallel to the biotite ages in the upper part of the profile, whereas towards the Insubric Line a significant deviation from the biotite age progression is attributed to tilting of the basement during the Oligocene. Zircon fission-track ages around 38 Ma are found close to the Insubric Line. No age offset, neither at the CMB nor at the Pogallo Line, is observed. This confirms the hypothesis that the Pogallo Line is an oblique normal fault, and that the CMB Line has accommodated only minor vertical displacement. The capture of the different cooling ages confirms the tilting of the Ivrea–Verbano Zone during the Neo-Alpine deformation and contradicts the tilting of the Ivrea–Verbano Zone during the Permian.

Introduction

The Ivrea–Verbano Zone (IVZ) is located between Locarno and Ivrea in the southern Alps of the Piedmont Region of Italy and the Swiss Canton of Ticino. Together with the adjacent Strona–Ceneri Zone, it was the first key region interpreted in terms of an exposed cross-section of the lower to middle continental crust (e.g. Berckhemer 1969; Mehnert 1975; Fountain 1976; Fountain & Salisbury 1981) (Fig. 1). However, the pre-Permian evolution of the region is still a matter of discussion (e.g. Hunziker & Zingg 1980; Schmid 1993; Handy *et al.* 1999; Vavra *et al.* 1996). Following its Palaeozoic tectonometamorphic history, the Ivrea crustal section has been exhumed to shallower crustal levels, tilted and emplaced into its present position. Over the last 20 years, a number of review articles were published on its metamorphic petrology and structural evolution (e.g. Zingg

From: SIEGESMUND, S., FÜGENSCHUH, B. & FROITZHEIM, N. (eds) *Tectonic Aspects of the Alpine-Dinaride-Carpathian System.* Geological Society, London, Special Publications, **298**, 45–68.
DOI: 10.1144/SP298.3 0305-8719/08/$15.00

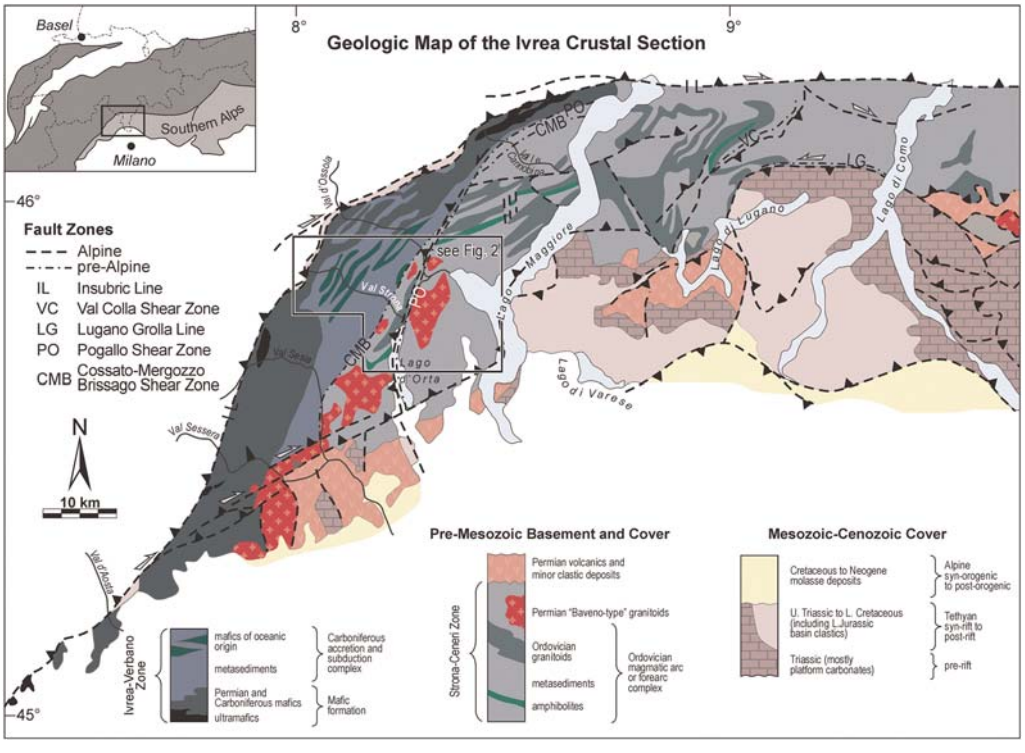

Fig. 1. Geological overview of the western part of the southern Alps (modified from Handy *et al.* 1999). The region consists of the metamorphic basement of the Ivrea–Verbano Zone (IVZ) and the Strona–Ceneri Zone (SCZ), and the Mesozoic to Cenozoic sedimentary cover. The outlined area around the Valstrona and Lago Maggiore was selected for structural and geochronological research (cf. Fig. 2).

et al. 1990; Boriani *et al.* 1990; Schmid 1993; Handy *et al.* 1999; Boriani & Giobbi 2004). In spite of this, the age, kinematics and geometry of the tectonic movements, which are responsible for exposing this almost complete crustal section at the Earth's surface, are the subject of ongoing debates (e.g. Handy & Zingg 1991; Schmid 1993; Handy *et al.* 1999).

Schmid *et al.* (1987) related the emplacement of the IVZ into its subvertical position adjacent to the Insubric Line to the Alpine orogeny, whereas Boriani *et al.* (1990) argued that vertical tilting took place prior to this, i.e. in the Permian. Handy *et al.* (1999) and Mulch *et al.* (2002) documented that the Strona Ceneri Zone (SCZ) was already moderately to steeply dipping in pre-Alpine times while the IVZ was tilted later, i.e. during the Late Oligocene to Early Miocene (Schmid *et al.* 1987).

Geochronological data are often used to constrain the timing and rates of geological processes, which are the major objectives in understanding the tectonic evolution of a region. In this study, the geochronology of a spectacular cross-section in the Valstrona di Omegna is presented (Fig. 2). This crustal section reveals different levels of the continental crust including granulite facies rocks in the NW and amphibolite facies in middle/upper crustal levels in the SE. Late Palaeozoic magmatism and its impact on the host formations is coeval at all crustal levels. This event is characterized by the emplacement of large mafic intrusions in the lower crust, resulting in the partial melting of metasediments and by plutonic and volcanic activity at higher crustal levels (e.g. Schmid 1978, 1979; Fountain 1986, 1989; Schmid 1993; Voshage *et al.* 1990; Rivalenti *et al.* 1975, 1981; Quick *et al.* 1994; Snoke *et al.* 1999; Peressini *et al.* 2007).

In order to bracket the exhumation history of the Ivrea Zone, dense sampling was performed in several field campaigns along the Valstrona profile (Fig. 2) and various minerals were geochronologically investigated. In this paper, we present new $^{40}Ar/^{39}Ar$ ages for hornblende, K–Ar ages on biotite and fission-track ages for zircon. Published U–Pb monazite ages (Teufel & Schärer *et al.* 1989; Henk *et al.* 1997) from almost identical sample localities along the Valstrona, as well as

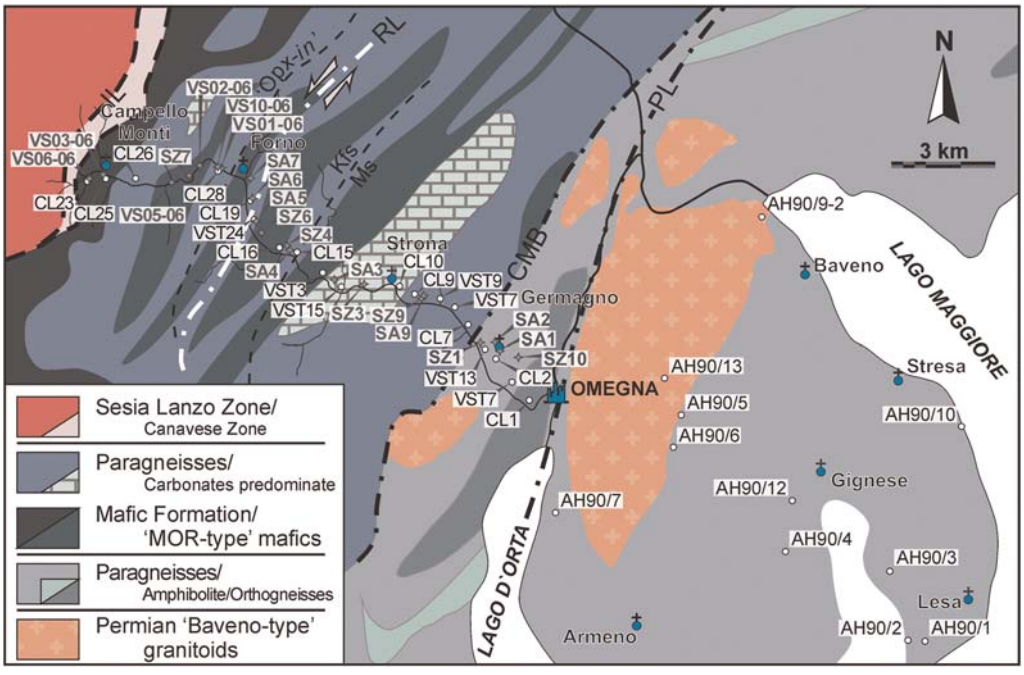

Fig. 2. Geology and sample sites along the Valstrona di Omegna–Lago Maggiore profile (modified after Bertolani 1969 and Handy *et al.* 1999). Sample sites for K–Ar Bt dating are indicated by open circles, whereas samples subjected to Ar–Ar Hbl and Zr fission-track dating are represented by grey stars.

published age data from other areas of the Ivrea Zone (Vavra *et al.* 1996; Boriani *et al.* 1990; Boriani and Villa 1997; Henk *et al.* 1997) are included to complete the dataset of the study. Together with available petrological data and structural field studies (Sills & Tarney 1984; Henk *et al.* 1997), we provide new constraints on the timing, kinematics and also to some extent on the displacement rates across distinct faults. The Rosarolo shear zone was selected to document the long-lasting time span and heterogeneity of deformation structures starting in the Permian.

Geological setting

The Ivrea Zone exposes a crustal section of the southern Alpine basement and is a SW–NE elongated body in the western Alps of Italy and Switzerland (Fig. 1). It is composed of the Ivrea–Verbano Zone (IVZ, 'formazione diorite-kinzigitica' by Novarese 1929) and the adjacent Strona–Ceneri Zone (SCZ, Serie dei Laghie of Boriani *et al.* 1990), and was the first region interpreted as an exposed cross-section of the entire continental crust (e.g. Berckhemer 1969; Mehnert 1975; Fountain 1976). The lowermost part of this section is often interpreted to represent the laminated lower crust, known from seismic sections all over the world. These are characterized by densely packed multiple sets of reflectors referred to as seismic lamellae (e.g. Fountain 1976; Burke & Fountain 1990; Rutter *et al.* 1993; Rabbel *et al.* 1998; Weiss *et al.* 1999).

The Ivrea Zone is separated from the Sesia Zone of the Central Alps by the greenschist facies Insubric mylonite belt (Fig. 1). The rocks tectonically incorporated into this mylonite belt are derived from the IVZ and the Sesia Zone, as well as from the Permo-Mesozoic sediments of the Canavese Zone. Shear criteria indicate that the mylonites accommodated back thrusting synchronous with back folding of the Central Alpine nappes. This was followed by a dextral strike-slip motion related to large transcurrent displacements in the Central Alps (Schmid *et al.* 1987).

The Pogallo Line, a 1–3 km-wide shear zone of mylonites, marks the subvertical contact between the SCZ and IVZ (Handy 1987). Hodges and Fountain (1984) first interpreted this shear zone in terms of a tilted normal fault of Mesozoic age. Boriani *et al.* (1990) identified the Cossato–Mergozzo–Brissagio Line (CMB-Line), which is closely associated with the Pogallo Line. The CMB Line (see Fig. 1) marks the transition between the IVZ and SCZ SW of the Val

d'Ossola, where the Pogallo Line breaks away from the lithological contact between these two basement units (see discussion in Schmid 1993 and Boriani & Giobbi 2004). The CMB Line is characterized as a Late Variscan strike-slip zone showing a spatial and temporary relationship with mafic and granitic igneous rocks, i.e. the Appinite Suite. The continuity of the metamorphic pressure gradient across the CMB Line indicates that the vertical displacement was negligible (Handy *et al.* 1999).

While residing in the lower crust, the amphibolite to granulite facies paragneisses of the IVZ were intruded by huge volumes of mafic to intermediate plutonic rocks, known as the Mafic Complex (Rivalenti *et al.* 1981; Voshage *et al.* 1990). Most prominent in the south, the Mafic Complex dominates the IVZ along its limit with the Sesia Zone of the Central Alps. In the north, it is comprised of numerous sill-like intrusions up to several hundred of metres thick, whereas in the south, particularly in the Val Mastallone, mafic rocks up to 10 km thick occur. Along the northwestern border of the Mafic Complex, in the vicinity of the Insubric Line, several ultramafic bodies crop out. They extend from Baldissero in the south to Finero in the north. The geochemical composition and P–T conditions characterize them as derived from continental mantle material (Rivalenti *et al.* 1975, 1981; Garutti *et al.* 1978/1979; Shervais 1978/1979; Voshage *et al.* 1988; Hartmann & Wedepohl 1993).

Mafic rocks that contribute to the metamorphic history of the IVZ are separated into three groups (Zingg *et al.* 1990; Schmid 1993): (i) mafics of oceanic origin alternating with paragneisses (Sills & Tarney 1984); (ii) large bodies of 'Anzola gabbro'-type mafics; and (iii) parts of the banded mafics within the granulite facies region of the IVZ such as those within the layered complex (Rivalenti *et al.* 1981). The mafic rocks predating the 270 Ma magmatic event comprise the gabbro-diorites of the Mafic Complex in the Valsesia (see discussion in Voshage *et al.* 1990). Pin (1986) reported concordant 285 Ma U–Pb ages of magmatic zircons for these diorites. More recently, Peressini *et al.* (2007) found that the magmatic activity was bracketed between 290 Ma and 288 Ma.

At a higher structural level, the central part of the IVZ, known as the Kinzingite Formation (Novarese 1929), becomes dominant. In the Valstrona crustal profile, amphibolite-facies metapelites (the so-called kinzigites) and minor amphibolites constitute the uppermost part of the profile, whereas granulite-facies metapelites (known as stronalites) and mafic rocks make up the lowermost part in close proximity to the Mafic Complex. The appearance of subordinate silicate marbles, pegmatites and microgranites has also been described by Bertolani (1969). The degree of metamorphism of the Kinzigite Formation increases from amphibolite facies conditions in the SCZ and the lower part of the IVZ to granulite facies conditions close to the Insubric Line (Zingg 1983; Sills 1984; Henk *et al.* 1997). According to Sills (1984), granulite-facies metamorphism in the metapelites from the NW section of the Strona Valley reached maximum P–T conditions of 750 ± 50 °C and 6 ± 1 kbar. Henk *et al.* (1997) found peak metamorphic conditions of 810 ± 50 °C and 8.3 ± 2.0 kbar for a metagabbro from the base of the Mafic Complex. The lowest metamorphic conditions were obtained from alumosilicate-bearing gneisses near Omegna in the SCZ with P–T conditions of 580 ± 30 °C and 2.3 ± 0.5 kbar (Henk *et al.* 1997).

The metamorphic pressure gradient across the IVZ is about 0.41 kbar/km in the Valstrona section. This implies significant crustal thinning, particularly in the lowermost 5 km of the crust (Henk *et al.* 1997). These authors estimated that about 4 km of crustal attenuation occurred during the Early Permian. This estimate is in agreement with observations made by Sills and Tarney (1984), whereas Brodie and Rutter (1987) inferred only 2 km of lower crustal thinning in the IVZ. A higher pressure gradient of 1.7 kbar/km in the Valle Cannobina, located in the NW of the Valstrona (Fig. 1), suggests heterogeneous stretching subparallel to the lateral extent of the IVZ, which is attributed to the activity of the Pogallo shear zone (Handy *et al.* 1999). Normal faulting at the low angle Pogallo shear zone took place between 180 and 230 Ma (Hodges & Fountain 1984; Handy 1987).

The timing of peak metamorphism is still a matter of discussion. SHRIMP U–Pb data from a magmatic zircon population, with crystal shapes characteristic of calc-alkaline magmatites, yield a crystallization age of 355 ± 6 Ma (Varva *et al.* 1996). The oldest metamorphic zircon rims in the metasediments of the IVZ are Early Permian (*c.* 296 Ma). In contrast, U–Pb ages for monazite and zircon from the SCZ point to a mid-Palaeozoic metamorphic event at *c.* 400 Ma (Köppel & Grünfelder 1978/1979; Köppel 1974; Rigaletti *et al.* 1994). A numerical simulation (Henk *et al.* 1997) of the temperature development in the IVZ, in response to the emplacement of the Mafic Complex, suggests that the metamorphic peak occurred prior to 300 Ma. The range of U–Pb monazite ages (assuming a closure temperature of *c.* 600 °C) between 272 Ma and 292 Ma document the heating pulses related to the magmatic underplating, which had created the typical granoblastic structure in the Ivrea Zone. Additional geochronological data for the IVZ recorded the

progressive cooling from the high temperatures prevailing during the Permo-Carboniferous metamorphic peak to temperatures of around 300 °C in the Jurassic (e.g. Zingg *et al.* 1990).

Results

Structural geology of the study area

Metamorphic foliation and banding in the IVZ are generally steeply inclined and trend NE–SW. An eastward plunge of stretching lineations is remarkably constant. Recently, Rutter *et al.* (2007) proposed that large-scale superimposed folding in the upper part of the IVZ in the Valstrona section occurred during regional migmatization, probably during the Hercynian orogeny. The IVZ in the Valstrona cross-section is bounded to the northwest by the Insubric mylonite belt. It is in contact with the adjacent SCZ to the southeast across the CMB Line (Boriani *et al.* 1990, see also Fig. 1). The CMB Line is considered to be a major subvertical tectonic discontinuity of Permian age (Boriani & Villa 1997; Mulch *et al.* 2002; or Boriani & Giobbi 2004). Starting in Permian times, the region was subjected to large-scale injection by basic magmas, accompanied by pervasive east–west stretching and crustal thinning of several kilometres. A network of conjugate high-temperature, low-angle shear zones in a layered lower crustal section related to this stretching has been identified (Brodie & Rutter 1987; Brodie *et al.* 1989, 1992; Rutter *et al.* 1993; Snoke *et al.* 1999). The corridor of shear zone outcrops, which passes through Anzola (Val d'Ossola) and Forno (Valstrona), can be traced for more than 20 km. The radiometric ages from the Anzola shear zone indicate that it relates to extension, which commenced prior to 280 Ma (Brodie *et al.* 1990), approximately coeval with the intrusion of the Mafic Complex. Metabasic rocks incorporated into inhomogeneous shear zones and transformed into mylonites and ultramylonites were deformed by dislocation creep accompanied by prograde dynamic recrystallization (Dornbusch & Skrotzki 2001).

The displacements along the CMB Line are clearly contemporaneous with the Permian mafic underplating events, and lead to the juxtaposition of the IVZ with the SCZ (Giobbi & Brodie 2004). The CMB mylonites are locally overprinted by a younger amphibolite to greenschist facies mylonite zone, the Pogallo Line. Mylonitization along the Pogallo Line clearly postdates the activity of the CMB in the Early Permian. The age of the Pogallo Line has been previously constrained to 160–240 Ma (Zing *et al.* 1990). In the Valstrona area, the Pogallo Line is only evidenced by brittle deformation due to the oblique low-angle normal fault geometry of the Pogallo Line, which has been reoriented in Alpine times (Handy 1987).

In the Valstrona cross-section, a long-term steeply inclined (present-day coordinates) shear zone is found, referred to as the Rosarolo shear zone (Fig. 2). The oldest high-temperature ultramylonites found in metabasic rocks can be related to the Anzola-type shear zones and incorporated mafic injections. At this time, the whole sequence was presumably in a horizontal position. The subsequent formation of pseudotachylites and other brittle deformation features took place within the upper crust. Shear sense criteria are principally sinistral, and antithetic shears only appear subordinate. The simplified sketches shown in Figure 3 illustrate that high-temperature mylonitization took place in the lower crust as part of an extensional fault system, while the evidence of frictional melting and brittle faulting indicates sinistral strike-slip movement in the middle and upper crust. In the following section, we describe the Rosarolo shear zone and argue in more detail to document the long time span and heterogeneity of deformation structures.

Fabrics of the Rosarolo shear zones

On the whole, the study area can be described as a high-strain shear zone. In its central parts, it consists of a network of sub-parallel anastomosing shear zones at the cm to m scale. Each of these minor mylonitic shear zones displays structures, which indicate that several strain increments occurred at different P/T conditions (Fig. 4). A large number of macro- and microstructures provide evidence that—with respect to present-day coordinates—sinistral shear operated over a long time span from the ductile to the brittle field (Ahrendt *et al.* 1990; Clausen 1990; see below). Only in a few cases are subordinate structures with an antithetic (dextral) sense observed. Because of distinct rheological contrasts between individual layers, which are mainly controlled by the ratio of mafic to felsic minerals, brittle and ductile deformation may also have operated more or less simultaneously. This resulted in a large variety of deformation structures and complex interactions of deformation processes. Macroscopically, the significance of rheological contrasts is best documented by ductile flow of felsic layers filling gaps produced by brittle faults affecting more mafic layers (Fig. 4b). Frequently, the common leucocratic segregations are cut by early formed mylonitic foliations, but were deformed and partly obliterated within the high strain cores of small-scaled shear zones (Fig. 4c).

Considering the shear zone as a whole, the mylonitic foliations are steeply inclined and strike NNW–SSE, grading into the NE–SW striking

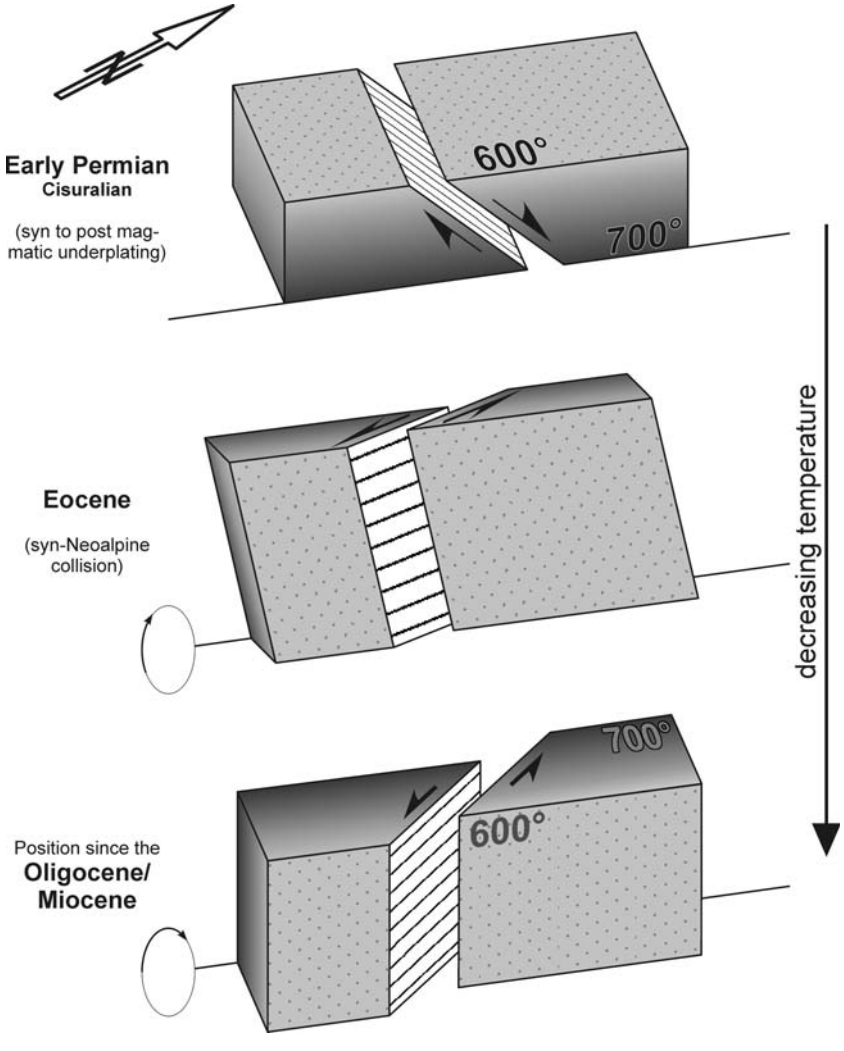

Fig. 3. Extensional tectonics in the lower crust resulting from the probable underplating of the mafic formation. The blocks were rotated during the Oligocene–Miocene uplift of the Ivrea basement and today appear as left lateral shear zones. Original vertical temperature profile now in a subhorizontal position.

metamorphic layering of the country rocks. This general sigmoidal trend of the foliations indicates a bulk sinistral sense of shear. In the central parts of the shear zone, the width of metapelitic layers is strongly reduced as compared to the more mafic lithologies. Locally, shear zones appear discontinuous because the main mylonitic foliation is transected by mylonitic horizons of different compositions. These probably represent former composite dykes (Fig. 5a) produced by crack-seal processes with alternating felsic and mafic input. Within the high strain area, the main brittle faults and the majority of associated pseudotachylites roughly follow the mylonitic foliation.

Boudin-shaped domains of comparatively low strain developed between the individual shear zones. Relics of early strain increments are also well preserved in these domains. Within the metabasic layers, a weak HT-mylonitization is indicated by fine-grained recrystallized rims around plagioclase and hornblende porphyroclasts. Around clinopyroxene, however, they are weakly developed. The orientation of the corresponding mylonitic foliation is strongly controlled by the metamorphic banding. Other often observed structures are boudins within mafic layers associated with tension or shear fractures, where the necking zones are filled with leucocratic segregations (Fig. 5b).

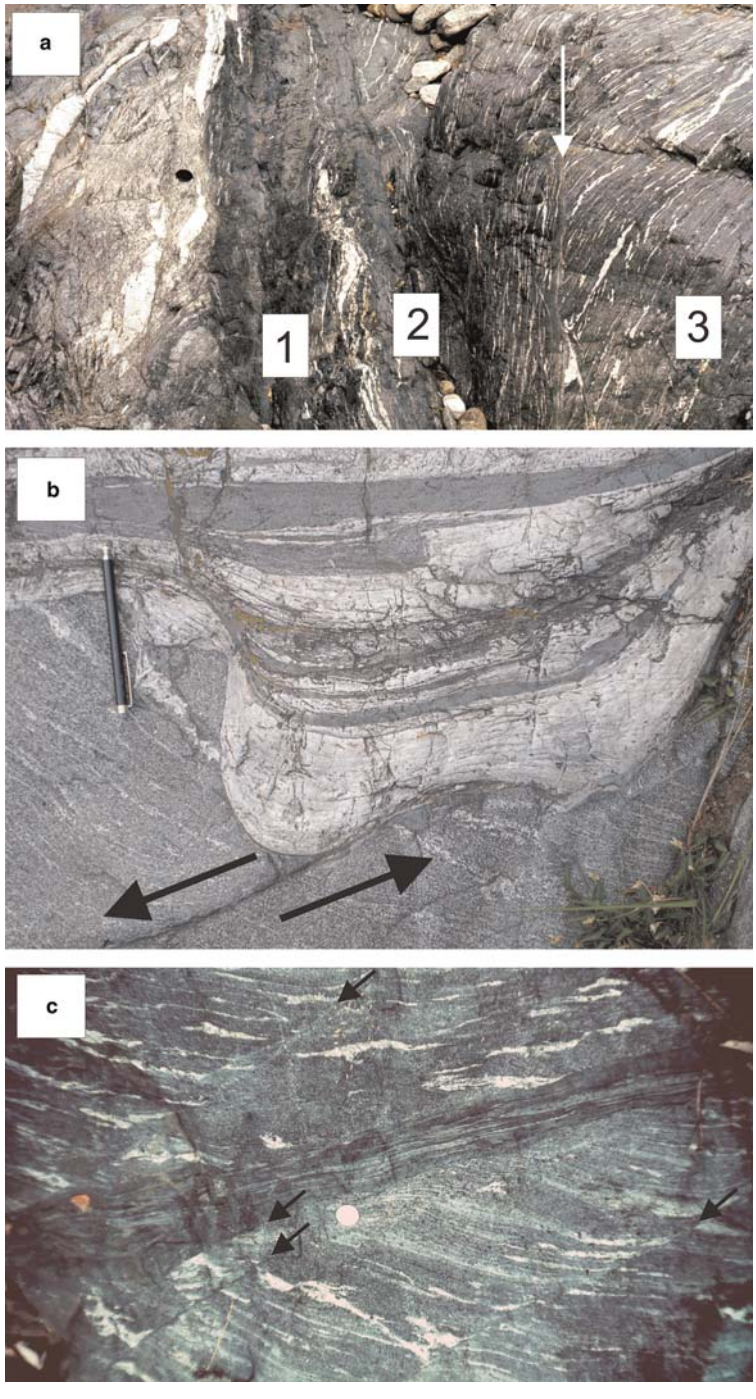

Fig. 4. Characteristics of the Rosarolo shear zone. (**a**) Complex structure of a polyphase shear zone at the metre scale. The dark ultramylonite (1) and cataclastic layers (2) form the core zone, with mylonitic country rock (3) in discontinuous contact to the shear zone core (arrow). (**b**) Ductile deformation of felsic layers, which probably originated from a composite dyke, filling a gap produced by a simultaneous shear fracture (see arrows). (**c**) Discontinuous shear zone at the dm scale. In the central high strain zone, the leucocratic injections are extremely stretched as compared to the mylonitic wall rock. Synthetic brittle–ductile shear planes (arrows) are developed at low angle to the central zone.

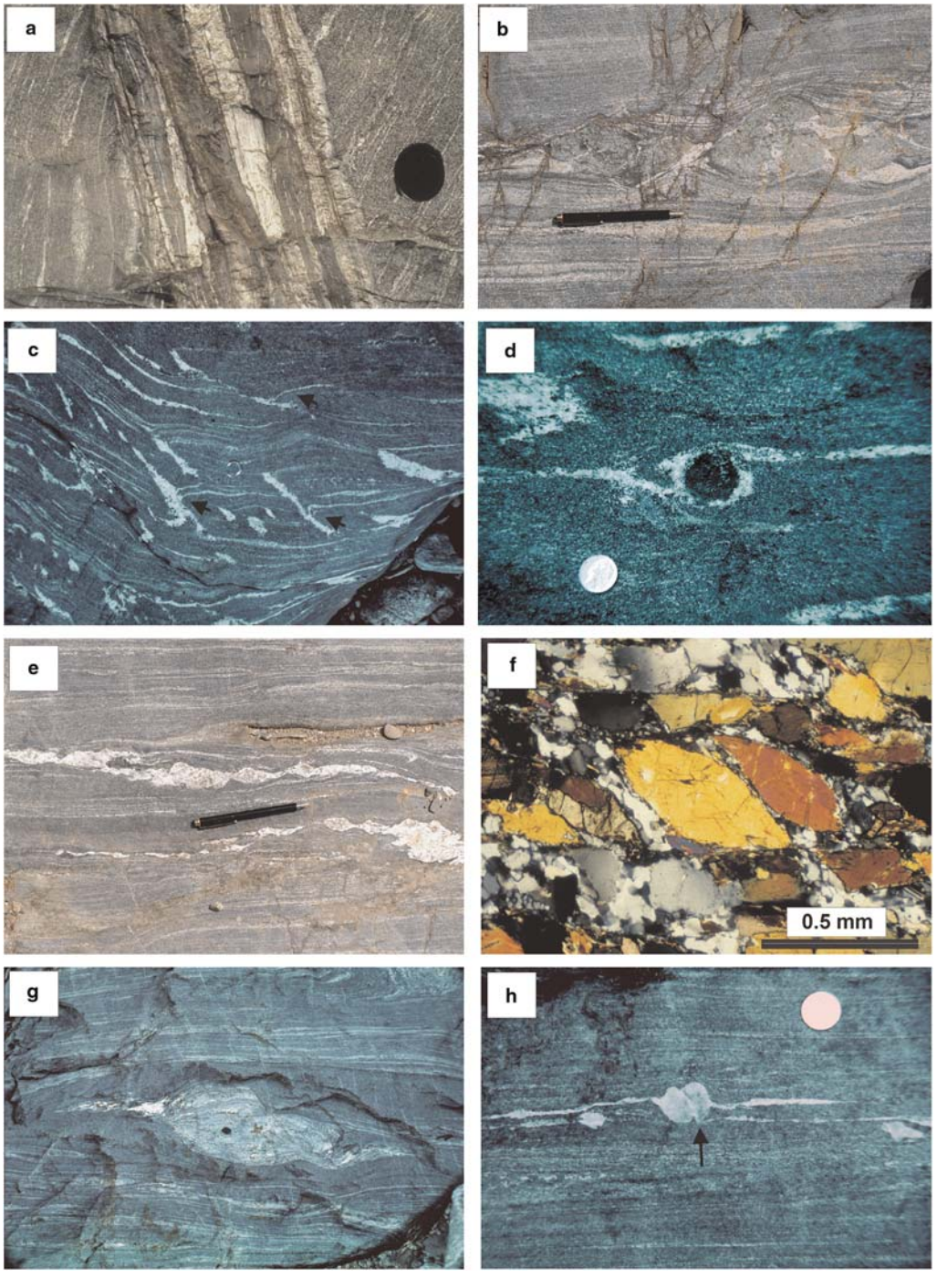

Fig. 5. Details of shear zone fabrics. (**a**) Finely laminated mylonite (left and right side) cut by a layered mylonite, which probably represents a former mylonitized composite dyke. (**b**) Synthetic sinistral shear fractures producing asymmetric boudinage of a mafic layer embedded in finely laminated mylonites; necking areas are filled with leucocratic injections. (**c**) Small-scale leucocratic veins within the mylonites, which are probably related to synthetic P-fractures, as indicated by dragging of the mylonitic foliation (arrows); locally the leucocratic veins are branched and form thin sills parallel to the mylonitic foliation.

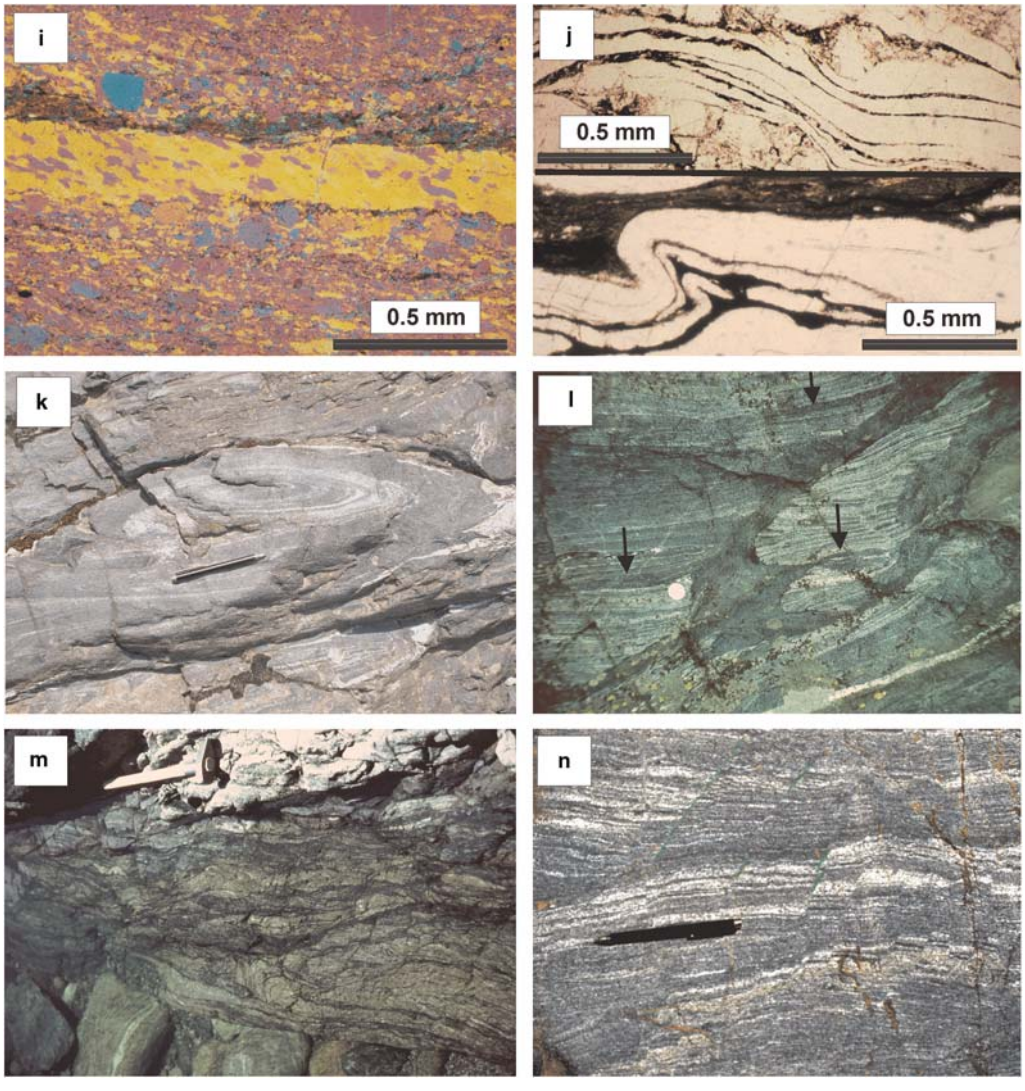

Fig. 5. (*Continued*) (**d**) Foliation-parallel leucocratic injection rotated together with a clinopyroxene porphyroblast/clast indicating a sinistral sense of shear. (**e**) Boudinage of a leucocratic segregation, which formed at a low angle to the mylonitic foliation; cores of boudins contain plagioclase porphyroclasts, while rims and necking zones consist of recrystallized aggregates. (**f**) SC-fabric displayed by hornblende 'fishes' and shape-preferred orientation of other constituents. (**g**) 'Litho-porphyroclast' (probably isolated boudin or remnant of a rootless intrafolial fold hinge); sigma-clast-like shape results from tails, which consist of stretched clast material and deformed segregations. (**h**) Brittle–ductile plagioclase porphyroclast with antithetic fragmentation and extremely long recrystallization tails. The tip of the right fragment (arrow) is affected by a continuing ductile deformation, which leads to the formation of a second generation recrystallization tail. (**i**) Mylonitic quartz layer displaying a distinct texture and shape-preferred orientation of grains, which indicate a sinistral sense of shear; crossed polars, with one quartz wave plate. (**j**) Mylonitic quartz layers separated by thin films of fine-grained material (top), which may indicate that the quartz layers were formed by repeated crack opening and healing parallel to the mylonitic foliation. Locally, these quartz layers also display asymmetric folds (bottom). (**k**) Elliptical cross-section of a sheath fold. (**l**) Mafic dyke, which cuts the mylonitic foliation or forms sills (arrows) parallel to it. (**m**) Cataclastic part of the shear zone containing fragments of the mylonitic host rock. (**n**) Set of planar sinistral fractures at the dm scale within the mylonites.

Typical structures along the less-deformed margin of the shear zone are synthetic P-faults (e.g. Logan *et al.* 1979), which are also filled with leucocratic injections (Fig. 5c). Dragging of adjacent layers gives evidence of sinistral shear along these planes. These veins are often connected with foliation-parallel segregations and occasionally were formed around larger porphyroblasts of clinopyroxene (Fig. 5d). Ductile deformation resulted in different kinds of boudinage, where other leucocratic veins formed both parallel or at low angle to the layering (Fig. 5e). The cores of these boudins often contain feldspar porphyroclasts, whereas recrystallized grains form the stretched areas. At the microscale, the sinistral sense of shear is best documented by SC-fabrics in mafic layers formed by 'hornblende fishes' together with corresponding oblique shape-preferred orientation of other components (Fig. 5f).

Individual layers contain small-scale lenses with complex fold structures (Fig. 5g), which may be interpreted as isolated relics of rootless hinge zones of intrafolial folds, which would imply localized high strain values. Along their boundaries, leucocratic segregations are emplaced, which partly are affected by ductile shear as indicated by asymmetric tails. Within these mylonites, isolated plagioclase porphyroclasts are embedded, which show both recrystallization tails and antithetic domino-like fracturing clearly indicating sinistral sense of shear (Fig. 5h). In many other comparable cases, however, the age relationships between ductile and brittle deformation remain questionable.

Within leucocratic horizons, quartz layers often display distinct textures associated with shape-preferred orientation obliquely inclined to the mylonitic foliation in a sinistral sense (Fig. 5i). These textures were qualitatively checked using a λ-plate pointed to the dominance of basal slip. Trails of solid opaque inclusions parallel to many of these quartz layers suggest that they originated by multiple crack healing parallel to the macroscopic layering (Fig. 5j).

Sheath folds appear at different dimensions ranging from the cm to m scale (Fig. 5k). They are related to an early HT deformation regime, because both mafic and felsic layers are homogeneously deformed.

During a late stage of the deformation history, irregular networks of mafic dykes intruded. These cut the mylonitic foliation or form short sills parallel to it (Fig. 5l). They are mainly composed of fine-grained recrystallized hornblende, partly containing relics of clinopyroxene, together with plagioclase and minor amounts of sphene. Locally, narrow bands of retrogressive biotite are interpreted as an incipient cleavage and represent the only macroscopic deformation feature.

Small cataclastic zones at the dm to m scale occur locally, which strike parallel to the central parts of the ductile shear zones. They mostly consist of lenticular fragments of the mylonitic country rock, which are embedded in an anastomosing network of narrow fractures filled with fine-grained gouge (Fig. 5m). The age relationship between these young cataclastic zones and the mafic dykes described above could not be determined, because cross-cutting structures of these two fabric elements were not observed.

Planar antithetic fractures at a high angle to the large-scale shear plane, which affect both felsic and mafic layers, can be attributed to late strain increments at low temperatures (Fig. 5n). In addition, brittle faults are developed which locally curve into the mylonitic foliation.

Several isotopic systems have been analyzed in order to constrain the age of metamorphism, the cooling history and the timing of the shearing.

Monazite U–Pb ages

Teufel & Schärer (1989) and Henk *et al.* (1997) presented 12 generally concordant U–Pb monazite ages from metasedimentary samples collected along the Valstrona cross-section (Fig. 2). From petrographic observations, it appears that the monazites are unzoned and oriented parallel to the main foliation. The monazite ages in the IVZ are all rather similar and ranging from 292 Ma to 276 Ma. Older (Caledonian) ages were detected in the SCZ (Fig. 6). In the IVZ, the ages become younger with increasing depth. This trend has been interpreted to reflect either cooling after regional metamorphism (Henk *et al.* 1997) or fluid circulation after the thermal peak of this metamorphism (Vavra *et al.* 1996).

$^{40}Ar/^{39}Ar$ hornblende dating

Eleven hornblende separates (Table 1, Fig. 7a, 7b) were dated at the Geochronology Laboratory of the Geophysical Institute of the University of Alaska Fairbanks (see Appendix 1 for analytical information). The samples were collected along the Valstrona di Omegna profile (Fig. 2).

With the exception of samples farthest from the Insubric Line (SA1, SA2, SA9; *c.* 270 Ma), showing concordance between isochron and plateau ages, all samples show considerable amounts of excess argon. This is especially true for samples (VS01-06, VS02-06, VS03-06 and VS05-06) in the vicinity (<4 km) of the Insubric Line, which have $^{40}Ar/^{36}Ar_i$ ratios between 1450 and 1900 showing the presence of considerable amounts of excess argon. None of the samples show a true plateau. The weighted average ages of

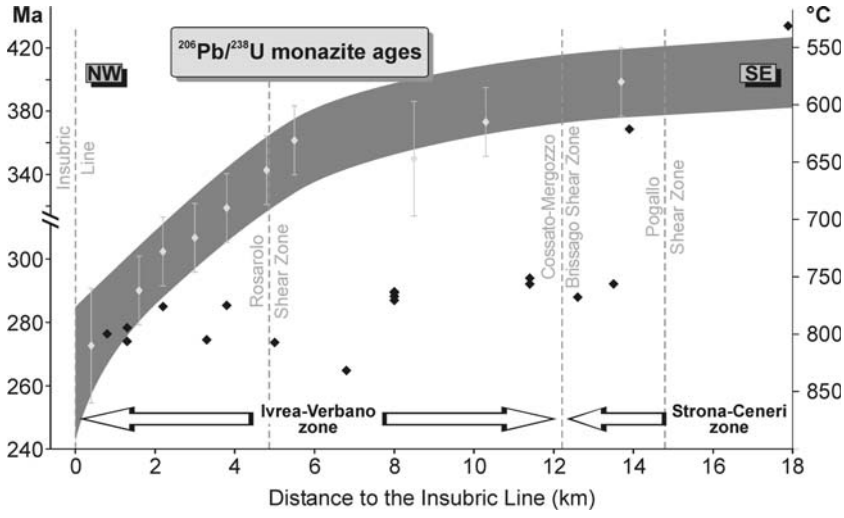

Fig. 6. Peak metamorphic temperatures (pale grey diamonds on grey trend) and U–Pb monazite ages (black diamonds) along the Valstrona section from the Insubric Line (0 km) to Omegna (*c*. 15 km). The data are taken from Henk *et al.* (1997) with one additional U–Pb monazite age from the SCZ of Grünfelder and Köppel (1971). Only the monazite ages in proximity to the Insubric Line can be explained by a complete reset of the U–Pb isotope system, whereas with distance the isotope system is only partly reset.

the youngest fractions averaging about 240 Ma, and the old integrated ages, are certainly biased by the excess argon. All four samples show well-defined isochrons with an average isochron age of 207.6 ± 2.3 Ma. The varying amounts of excess argon seen in these and other samples indicate open-system behaviour, and thus the isochron age is favoured in most cases (see Table 1). Isochron ages show a well-defined age progression becoming younger toward the Insubric Line (Fig. 7a).

K–Ar biotite ages

Another constraint on the cooling of the Ivrea Zone is gained from K–Ar biotite ages. Biotite separates were obtained from 30 metasedimentary rocks and measured at the K–Ar laboratory in Göttingen (see Appendix for analytical information). Of those samples, 19 correspond to the Valstrona whereas another 11 samples document the cooling history of the SCZ between the Lago d'Orta and Lago Maggiore (Table 2 and Fig. 8). Sample localities along the Valstrona largely correspond to the monazite samples of Henk *et al.* (1997) (Fig. 2). The K–Ar biotite ages continuously become younger from the SE to the NW, i.e. from the SCZ towards the IVZ. Lower Triassic ages (*c*. 245 Ma) were recorded in the SCZ near the Pogallo Line. Towards the Insubric Line, youngest ages are Late Jurassic, around 156 Ma, at the base of the IVZ. These data illustrate the migration of the zone of partial Ar retention in biotite, documenting the progressive cooling of the lower crust.

The trend of increasing K–Ar biotite ages advances in the direction of Lago Maggiore, where maximum ages of 335 Ma were recorded at the lakeside in the proximity of Lesa (Fig. 8). This profile also includes cooling ages of the Baveno granite scattering between 291 ± 7 Ma and 284 ± 7 Ma.

Zircon fission-track ages

The late stage of the cooling history is documented by zircon fission-track data for nine samples (see Appendix for analytical information). Analytical data are given in Table 3 and Figure 9. Only three of the nine dated samples passed the chi-square test, indicating that the single-grain ages do not form a normal distribution within the samples. The oldest, Lower Jurassic age of *c*. 178 Ma (SZ 10) is observed in the SCZ near the Pogallo Line, whereas the deepest part of the crustal section in the vicinity of the Insubric Line yielded Late Eocene ages of *c*. 38 Ma (VS 06-06, SZ 3).

Discussion

The new age data on the Valstrona cross-section together with the previously published work allow us to assemble an outline of the exhumation and deformation history of the region.

Table 1. *Hornblende data**

Sample	Distance to I.L. (km)	Integrated age ± 1σ (Ma)	Plateau (P) or weighted mean (W) age			Isochron (I) or errorchron (E) age			Ca/K
			Age ± 1σ (Ma)		Plateau information	Age ± 1σ (Ma)		Isochron information	
VS03-06	0.3	279.6 0.8	244.5	13.1	3 fractions (**W**) 71% ^{39}Ar release MSWD = 290.2	**201.7**	**13.0**	6 fractions (**E**) $^{40}Ar/^{36}Ar_i = 1453 \pm 326$ MSWD = 22.9	7.7
VS05-06	2.0	271.4 0.8	242.7	1.7	3 fractions (**W**) 56% ^{39}Ar release MSWD = 4.3	**210.3**	**4.4**	6 fractions (**I**) $^{40}Ar/^{36}Ar_i = 1624 \pm 144$ MSWD = 1.6	8.2
VS02-06	3.0	277.5 0.8	232.8	3.1	4 fractions (**W**) 73% ^{39}Ar release MSWD = 7.0	**206.1**	**3.0**	8 fractions (**I**) $^{40}Ar/^{36}Ar_i = 1903 \pm 133$ MSWD = 2.3	6.5
VS01-06	3.5	257.2 0.8	239.5	4.8	5 fractions (**W**) 78% ^{39}Ar release MSWD = 33.7	**211.1**	**7.0**	9 fractions (**E**) $^{40}Ar/^{36}Ar_i = 1743 \pm 271$ MSWD = 3.3	13.6
SA7	4.0	254.5 0.8	250.4	0.9	5 fractions (**P**) 73% ^{39}Ar release MSWD = 1.5	**222.7**	**12.5**	8 fractions (**I**) $^{40}Ar/^{36}Ar_i = 1337 \pm 445$ MSWD = 1.5	19.4
SA6	4.5	225.0 0.6	**221.9**	**0.6**	6 fractions (**W**) 94% ^{39}Ar release MSWD = 3.0	221.6	1.2	7 fractions (**E**) $^{40}Ar/^{36}Ar_i = 327 \pm 60$ MSWD = 4.8	6.5
SA5	5.5	294.8 0.8	261.9	0.9	3 fractions (**P**) 66% ^{39}Ar release MSWD = 0.1	**240.0**	**2.0**	5 fractions (**I**) $^{40}Ar/^{36}Ar_i = 1177 \pm 52$ MSWD = 2.1	9.9
SA4	6.5	284.6 0.8	246.7	1.5	1 fraction saddle (**W**)	**239.3**	**4.6**	5 fractions (**I**) $^{40}Ar/^{36}Ar_i = 702 \pm 118$ MSWD = 2.3	12.8
SA3	8.0	399.6 1.1	281.7	4.7	3 fractions (**W**) 44% ^{39}Ar release MSWD = 14.4	**250.4**	**3.7**	10 fractions (**E**) $^{40}Ar/^{36}Ar_i = 777 \pm 23$ MSWD = 7.2	15.4
SA9	10.5	264.2 0.9	**256.6**	**1.1**	5 fractions (**W**) 37% ^{39}Ar release MSWD = 2.8	261.2	9.9	5 fractions (**E**) $^{40}Ar/^{36}Ar_i = 445 \pm 308$ MSWD = 12.6	
SA2	12.5	265.0 0.8	**267.7**	**1.0**	3 fractions (**P**) 57% ^{39}Ar release MSWD = 1.3	269.5	2.0	6 fractions (**E**) $^{40}Ar/^{36}Ar_i = 180 \pm 26$ MSWD = 7.9	15.5
SA1	13.0	274.9 0.7	**271.1**	**0.7**	5 fractions (**P**) 84% ^{39}Ar release MSWD = 0.6	271.5	0.8	5 fractions (**I**) $^{40}Ar/^{36}Ar_i = 266 \pm 18$ MSWD = 0.6	13.2

*__Bold__: Preferred age for each sample (ages reported at ± 1 sigma).
Plateau: 3+ consecutive fractions, MSWD < *c*. 2.5, more than *c*. 50% ^{39} Ar release. If a group of fractions does not meet these criteria, a weighted average age is calculated. Isochron: MSWD < *c*. 2.5, otherwise it is considered an errorchron age.

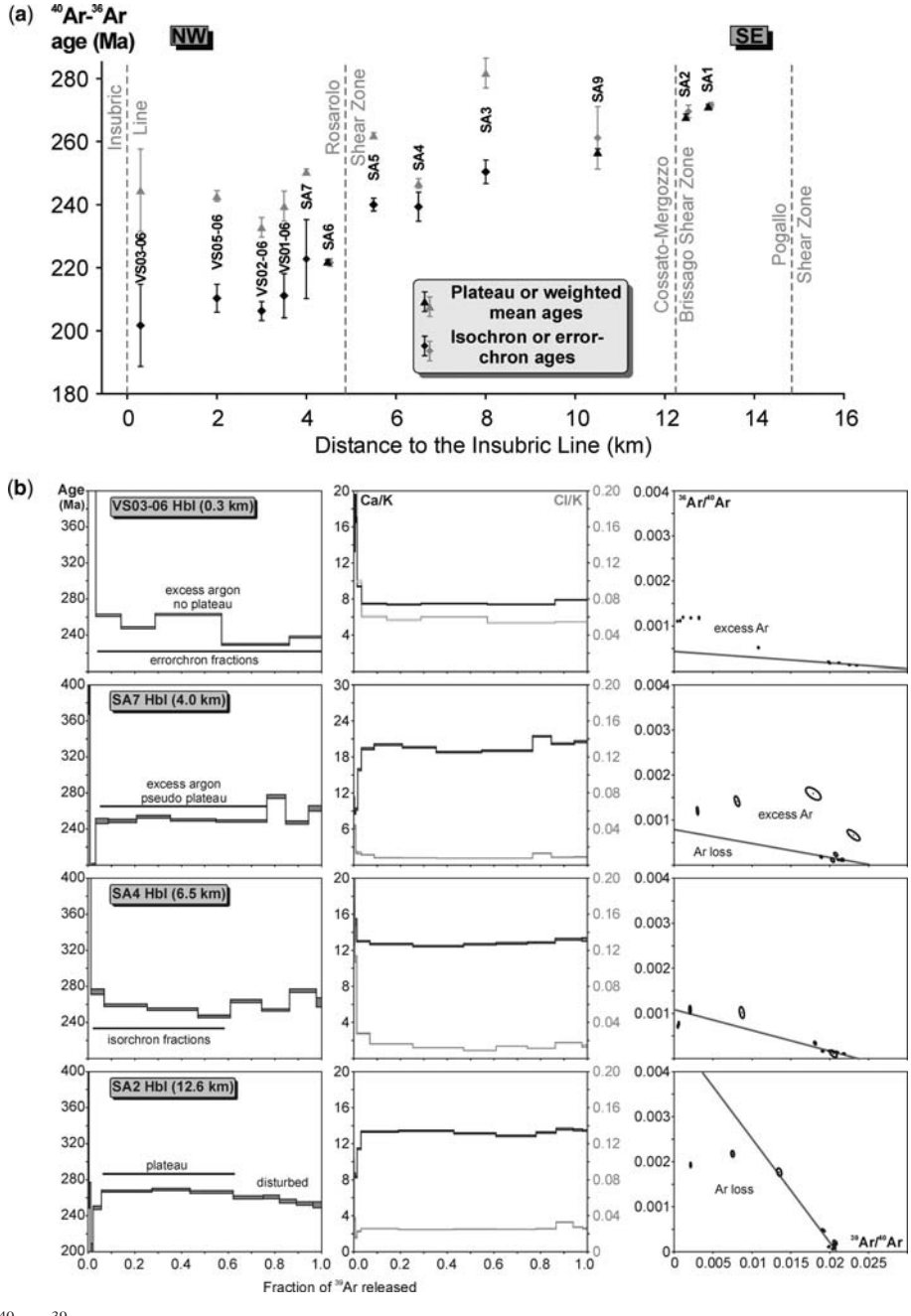

Fig. 7. $^{40}Ar-^{39}Ar$ hornblende data along the Valstrona. (**a**) Age versus distance to the Insubric Line relationship. Black symbols either corresponding to plateau and weighted mean ages (triangles) or isochron and errorchon ages (diamonds) are the preferred results of the data set. No age step is observed across the Cossato–Mergozzo–Bissago (CMB) shear zone suggesting a common cooling history of the IVZ and SCZ. (**b**) Age spectra of four representative hornblende analyses are shown. Besides the age information, i.e. heating step and isochron diagrams, the Ca/K and Cl/K ratios that might aid in the interpretation of the Ar analyses are presented. For the entire data set of the 12 analysed samples, the reader is referred to the online supplementary data at http://www.geolsoc.org.uk/SUP18311.

Table 2. *Compilation of the K/Ar biotite ages along the Valstrona–Lago Maggiore profile. The quoted errors comply with 95% of the confidence level (2σ). Ar-isotopic abundance: ^{40}Ar: 99.6000%; ^{38}Ar: 0.0630%; ^{36}Ar: 0.3370%. Spike—isotopic composition: ^{40}Ar: 0.0099980%; ^{38}Ar: 99.9890000%; ^{36}Ar: 0.0009998%. Decay constants (1/a): λε: 5.81×10^{-11}; λβ-: 4.962×10^{-10}; λtot: 5.543×10^{-10}. Potassium: ^{40}K: 0.011670%; K_2O/K: 0.8302. Standard temperature pressure (STP): 0 °C, 760 mmHg; Normal atmosphere (DIN 1343): 273.15 K, 1013.25 mbar. Molar volume (ml): 22413.8; Atomic weight (g/mol): ^{tot}Ar: 39.9477; ^{40}Ar: 39.9624; ^{tot}K: 39.1027.*

Sample	Mineral	Distance to I.L. (km)	K_2O (wt. %)	$^{40}Ar^*$ (nl/g)STP	$^{40}Ar^*$ (%)	K–Ar age ± 2σ (Ma)		± 2σ (%)
CL 23	bt	0.00	10.32	54.32	98.01	**156.3**	**3.3**	2.1
CL 25	bt	0.35	10.18	54.54	98.17	**159.0**	**3.4**	2.1
CL 26	bt	1.09	9.58	51.79	98.23	**158.7**	**3.3**	2.1
CL 28	bt	3.51	9.66	57.44	99.00	**175.7**	**3.7**	2.1
CL 19	bt	4.60	9.56	53.78	98.38	**166.6**	**3.5**	2.1
VST 24	bt	5.03	9.92	56.93	98.56	**169.8**	**3.6**	2.1
CL 16	bt	6.14	9.21	57.27	98.95	**183.3**	**3.8**	2.1
CL 15	bt	6.54	8.67	48.98	98.66	**167.3**	**3.5**	2.1
VST 3	bt	7.57	9.38	56.93	97.16	**179.1**	**3.8**	2.1
VST 15	bt	8.27	8.77	55.24	99.40	**185.5**	**3.9**	2.1
CL 10	bt	9.60	8.61	59.21	98.99	**201.7**	**4.2**	2.1
CL 9	bt	10.14	9.11	62.19	99.83	**200.3**	**4.2**	2.1
VST 9	bt	10.69	8.63	68.73	99.15	**231.6**	**4.8**	2.1
VST 7	bt	11.51	8.79	63.70	99.05	**211.9**	**4.4**	2.1
CL 7	bt	12.00	5.90	46.14	97.64	**227.6**	**4.9**	2.2
VST 13	bt	12.66	9.45	76.58	99.22	**235.4**	**4.9**	2.1
CL 2	bt	13.22	9.20	70.70	98.39	**223.9**	**4.7**	2.1
VST 5	bt	13.97	9.45	74.77	99.51	**230.2**	**4.8**	2.1
CL 1	bt	14.53	9.51	80.27	99.31	**244.5**	**5.1**	2.1
AH 90/7	bt	18.01	8.46	73.51	98.20	**251.2**	**5.3**	2.1
AH 90/13	bt	20.92	8.37	82.87	99.27	**283.7**	**7.4**	2.6
AH 90/6	bt	22.53	8.20	83.39	99.80	**290.8**	**7.2**	2.5
AH 90/9-2	bt	22.53	7.99	79.82	98.72	**286.0**	**6.9**	2.4
AH 90/5	bt	22.85	8.29	82.11	99.60	**283.8**	**6.1**	2.1
AH 90/12	bt	30.23	8.86	99.31	99.56	**318.0**	**6.6**	2.1
AH 90/4	bt	30.91	8.99	107.28	99.45	**336.8**	**6.8**	2.0
AH 90/3	bt	36.82	8.32	89.48	94.73	**306.2**	**7.1**	2.3
AH 90/10	bt	37.61	8.14	94.81	99.04	**329.4**	**7.1**	2.2
AH 90/2	bt	39.23	8.09	95.94	99.33	**334.8**	**6.8**	2.0
AH 90/1	bt	39.61	7.83	92.87	99.85	**334.9**	**7.0**	2.1

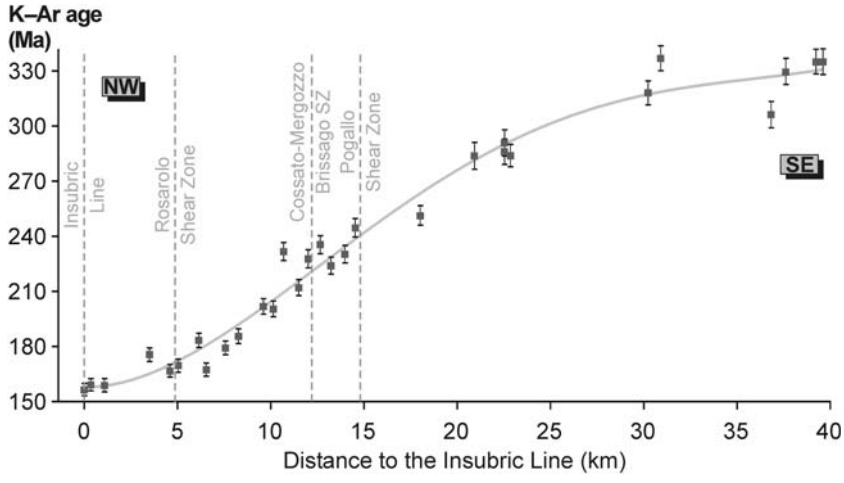

Fig. 8. K–Ar Bt ages between the Insubric Line (0 km) and Lago Maggiore (*c*. 40 km). Besides the IVZ, the profile also includes the K–Ar Bt cooling ages for the Strona Ceneri Zone (cf. Fig. 2 and Table 3). No abrupt steps of the cooling ages are observed across the two tectonic lines, i.e. the Cossato–Mergozzo–Bissago and Pogallo shear zones.

Significance of the geochronological data

Since the early work by Wagner *et al.* (1977), the estimated closure temperature interval of the U–Pb system in monazite has shifted significantly from 550 °C up to 650–725 °C (Copeland *et al.* 1988; Parrish 1990; Metzger *et al.* 1991). Kamber *et al.* (1998) even proposed a closure temperature in excess of 800 °C. The conditions leading to monazite growth in metamorphic rocks are poorly understood (Lanzirotti & Hanson 1996; Sawka *et al.* 1986; Bonn 1988; Seydoux-Guillaume 2001). Bonn (1988) and Milodowski & Hurst (1989) demonstrated that monazites may grow under greenschist facies or even during diagenetic conditions.

The peak of the granulite facies metamorphism in the IVZ was attained at *c*. 300 Ma (or earlier). This is based on the finite element approximation of thermal simulations by Henk *et al.* 1997, assuming a monazite closure temperature at 600 ± 50 °C (Smith & Barreiro 1990). In the amphibolite facies rocks (northwest and southeast of the CMB Line in Figs 1 and 6), the age of metamorphism is dated at *c*. 292 Ma (Henk *et al.* 1997). The high estimate of the monazite closure temperature by Kamber *et al.*

Table 3. *Zircon fission-track ages obtained on gneiss samples of the Valstrona di Omegna profile across the Ivrea body. Cryst: number of dated zircon crystals. Track densities (RHO) are as measured ($\times 10^5$ tr/cm^2); number of tracks counted (N) shown in brackets. Chi-sq P(%): probability obtaining Chi-square value for n degree of freedom (where n = no. crystals-1). Disp.: Dispersion, according to Galbraith & Laslett (1993). *: Central ages calculated using dosimeter glass: CN2 with $\zeta_{CN2\text{-}zircon} = 127.8 \pm 1.6$*

Sample	Distance to I.L. (km)	Cryst.	RhoS	(Ns)	RhoI	(Ni)	RhoD	(Nd)	Chi-sq. P (%)	Disp.	Central age ±1σ (Ma)	
VS 06-06	0.2	20	49.65	(859)	55.89	(967)	6.629	(4859)	4	0.16	**37.7**	**2.3**
SZ 3	3.0	18	47.90	(904)	52.56	(992)	6.631	(4859)	2	0.17	**38.2**	**2.5**
VS 10-06	4.5	20	80.51	(1195)	59.76	(887)	6.627	(4859)	0	0.23	**56.8**	**4**
SZ 4	6.0	20	83.73	(1251)	39.82	(595)	6.622	(4859)	53	0.01	**88.4**	**4.7**
SZ 6	6.5	15	95.19	(1048)	41.87	(461)	6.597	(4859)	0	0.27	**97.1**	**9**
SZ 7	8.5	20	123.51	(1979)	41.07	(658)	6.624	(4859)	84	0	**126.1**	**6.2**
SZ 9	10.5	15	126.33	(1515)	35.69	(428)	6.62	(4859)	0	0.29	**151.5**	**14.4**
SZ 1	13.0	20	159.80	(2372)	40.02	(594)	6.603	(4859)	54	0.02	**166.3**	**8.3**
SZ 10	13.8	21	217.20	(2199)	48.89	(495)	6.615	(4859)	0	0.24	**180.1**	**13.4**

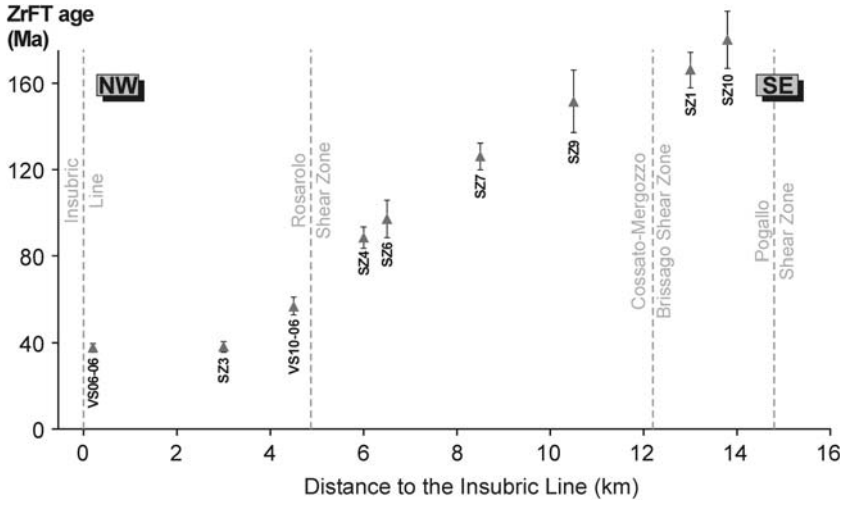

Fig. 9. Apparent zircon fission track data along the Valstrona profile (cf. Table 3). Note the distinct bend of the data trend at *c*. 3 km distance to the Insubric Line. A less-pronounced bend also occurs in the southeast of the Cossato–Mergozzo–Bissago (CMB) shear zone.

(1998) and the peak metamorphic temperatures (Sills & Tarney 1984; Henk *et al.* 1997) impede a straightforward interpretation of the monazite ages as either cooling or growth ages. The available U–Pb monazite ages (Henk *et al.* 1997) show a systematic decrease from 292 $\pm$ 2 Ma near the Pogallo Line to 276 $\pm$ 2 Ma at the base of the IVZ indicating younger ages for the granulite facies sequence. When assessing the role of multiple and long-lasting magmatic underplating with respect to the discussed P–T conditions (Zingg 1983; Sills & Tarney 1984; Henk *et al.* 1997), considering the above-discussed new closure temperature for U–Pb in monazite, the significance of the monazite ages may change. First, the elevated isotherms were only slightly affected (if at all) by the magmatic underplating. The SCZ provides an explanation for the ages (*c*. 292 Ma) in proximity to the Pogallo Line (see Fig. 7). The repeated heat input by the intrusion of mafic melts up to *c*. 285 Ma (Pin 1986; Peressini *et al.* 2007) or even longer (Voshage *et al.* 1990) was sufficient to reset the monazite U–Pb isotope equilibrium in the deeper parts of the IVZ explaining the younger ages. The long-lasting magmatic activity is also corroborated by 261 $\pm$ 4 Ma U–Pb SHRIMP ages on zircons from anatectic leucosomes in the IVZ metapelites (Vavra *et al.* 1996). However, the question arises whether the oldest monazite ages are already a result of reset due to the underplating.

The validity of the proposed 'closure temperature' of monazite of 800 °C or 725 °C can be easily constrained by the $^{40}Ar/^{39}Ar$ hornblende ages (see Figs 7 and 10). Following Dahl (1996) and Villa *et al.* (1996), the lower limit of the closure temperature of recrystallization-free amphiboles with values for Z = 38.1% (Z as defined by Dahl 1996) is $\geq$550 °C. Kamber *et al.* (1995) reported a temperature of 580 °C assuming a cooling rate of 1–2 °C/Ma. Boriani & Villa (1997) reported Z-values between 37.7% and 38.4% for amphiboles of the SCZ suggesting that at least the lower limit of the closure temperature interval is covered. The amphiboles of the SCZ and also within the amphibolite facies part of the IVZ have to be considered as formation ages dating the metamorphic peak at temperatures higher than 550 °C (e.g. Zingg 1983; Henk *et al.* 1997).

The $^{40}Ar/^{39}Ar$ hornblende ages and K–Ar biotite ages (Tables 1, 2 or Figs 7, 8 and 10) are interpreted to reflect the time of cooling of the crust after Permian heating caused by mafic intrusions. The closing temperature for hornblende should be around 500–600 °C (McDougall & Harrison 1999), while that for biotite can range between the extreme values of 300° $\pm$ 50 °C for simple cooling (Purdy & Jäger 1976; McDougall & Harrison 1999) and 450 °C for the total reset of the K–Ar system in recrystallization-free minerals (cf. Villa 1998). In this case, the lower closing temperature seems to be more appropriate assuming that the biotites in the vicinity of the Insubric Line behaved as open systems before and during the Permian heat flow.

The decrease of ages towards the rocks of a formerly deeper position simply reflects slow

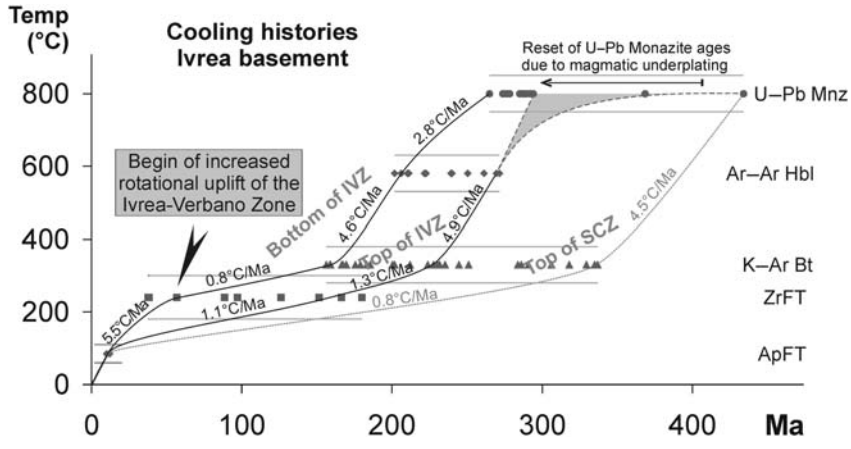

Fig. 10. Thermal history over the last 400 Ma for the Strona–Ceneri Zone and for the Ivrea–Verbano Zone.

exhumation. Permian or older hornblende and biotite cooling ages originate from rocks with a significantly higher crustal position before the late-stage tilting. Therefore, the whole transect represents a single trend. From the Valstrona section, we cannot find any indication for different cooling histories influenced by any movements along the Pogallo Line or the CMB Line. A comparable tendency may be assumed for the zircon FT ages which are only affected in the vicinity of the Insubric Line, indicating the beginning of an increased rotational uplift of the IVZ at around 40 Ma.

Thermal history–age of tilting

The obtained geochronological data from the Valstrona transect convey a certain amount of information on its tilting. Boriani *et al.* (1990) considered this process to be of Permian age, while Schmid *et al.* (1987) argued for an Eocene to Miocene age. Handy *et al.* (1999) found structural evidence indicating that the two crustal sections were rotated at different times: (1) the IVZ was tilted into its upright position during the Oligocene; and (2) the SCZ was already moderately steeply dipping.

The thermal history can be summarized as follows: the Permian underplating of mafic melts into the lower crust of the Ivrea section and the subsequent extension of the basement led to a pervasive heating, and partial or complete equilibration of, the U–Pb monazite isotope system between the Pogallo Line and Insubric Line in the Valstrona profile. Further to the SE, Caledonian ages are recorded, turning emphasis on the importance of the CMB Line during the Late Palaeozoic, when it acted as an extensional detachment facilitating the ascent of the mafic melts towards higher crustal levels (e.g. Mulch *et al.* 2002). Peak metamorphic conditions gained during the emplacement of the mafic melts reached 810 °C and 8.3 kbar (Henk *et al.* 1997).

Thermal simulations by Henk *et al.* (1997), using an uplift rate of 0.4 mm/a for 10 Ma, indicate that the disturbance of isotherms will persist for slightly longer than 5 Ma. Only when considerably higher peak metamorphic temperatures (>1000 °C) are assumed, will the thermal anomaly fade away after around 20 Ma. In this way, the obtained Ar–Ar ages that are at least 20 Ma younger (when plateau ages are considered) than the corresponding U–Pb monazite ages could be perturbed by the thermal impact of the mafic intrusion as well. Moreover, the careful evaluation of the analytical results favours the Ar–Ar isochron ages for the samples in proximity to the Insubric Line at *c*. 210 Ma that are certainly beyond the time interval of the thermal impact. Therefore, the $^{40}Ar-^{36}Ar$ hornblende ages in the range between *c*. 270 Ma in proximity to the Pogallo and CMB Lines and *c*. 210 Ma at the deepest section of the profile are attributed to the regional cooling and exhumation of the Ivrea basement during Permian and Triassic times.

The majority of Ar and zircon FT ages of the profile are apparent ages for the time span between the Permian and Eocene. They formed in a relatively stable crust that experienced high heat flow during the Triassic to Jurassic rifting phases. At first glance, the shifts of Ar and zircon FT ages along the profile suggest a long-lasting, monotonous cooling process that started in the Permian and lasted through the entire Mesozoic era until the Palaeogene. However, this interpretation has to be rejected, because it contradicts the known evolutionary history of the southern Alps. The stratigraphic record suggests a calm, continental

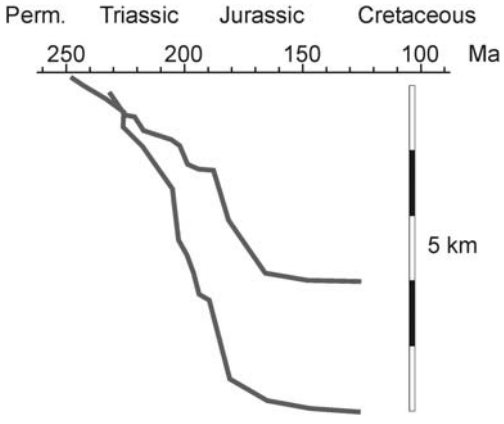

Fig. 11. Subsidence history of the southern Alps (from Stämpfli *et al.* 2002). The most intense extension happened during Early Jurassic time, between *c*. 200 and 175 Ma.

sedimentation for the post-Permian time (e.g. Stämpfli *et al.* 2002) until the mid-Triassic, and later an intense subsidence with alternating rift and basin facies development on the horst and graben structures formed by continental extension (see Fig. 11, Bertotti 1991). The Late Triassic and Jurassic crustal extension created a period of high heat flow in the southern Alps. Thus, the supposed exhumation for the western southern Alps during the Mesozoic is in sharp contradiction with the facts of sedimentation and structural records.

The hornblende $^{40}Ar/^{39}Ar$ ages (Fig. 7) show a monotonous trend of increasing isochron ages from 3.5 km towards higher crustal levels at the Pogallo Line. The oldest $^{40}Ar/^{39}Ar$ data, far from the Insubric Line, are practically identical to the mean of the monazite U–Pb ages. Thus, in that crustal level (the highest part of the profile), the post-Permian thermal pulses were not able to reset the Ar system of the hornblende. The very remarkable difference between the monazite ages and the youngest hornblende $^{40}Ar/^{39}Ar$ ages close to the Insubric Line indicates that the deepest part of the profile experienced a relatively high temperature of $>550\,^{\circ}C$ at least until Triassic times. These hornblende ages, at *c*. 210 Ma, point to the beginning of extension-induced subsidence in the Lombardian basin.

The biotite K–Ar ages ranging between 230 and 156 Ma run parallel to the hornblende ages in the upper part of the profile. A minor shift to a shallower trend is located about 8 km from the Insubric Line (Fig. 12). No abrupt offset of the decreasing age profile is observed across the two tectonic lineaments located in the lower part of the profile, i.e. the CMB and the Pogallo shear zones. This suggests that Mesozoic tectonism affected the entire basement pile in a uniform way. This trend is typical in exhumed argon retention zones, as was documented by Kamp *et al.* (1989) for the southern Alps of New Zealand, where, similar to the Ivrea Zone, the former reset zones of the different chronometers were exhumed with different metamorphic mineral assemblages.

The slope recorded between 15 and 8 km of the profile forms the base of the preserved partial argon retention zone. Below this zone (between *c*. 8 and 0 km on the profile), the trend has a high angle, and we interpret this section as the former depth of zero argon ages. The partial retention zone was formed at the end of Mesozoic rifting. The *c*. 160 Ma age of the break-in-slope corresponds well to the end of the intense rifting documented by the subsidence curves of the southern Alps (see Fig. 11).

The oldest zircon FT ages (Fig. 12) were measured in the highest part of the profile, above the depth of the break-in-slope of the biotite K–Ar age trend. The oldest zircon ages correspond well to the supposed reset history of biotite ages. The partial annealing zone (PAZ, namely the oblique section of the zircon ages) occupies a deeper position than the partial retention zone of argon ages. This PAZ was formed later, in post-Jurassic (post-rift) times, probably during and after the sinking and stabilization of the perturbed isotherms. The lower break-in-slope (4 km on the profile, *c*. 50 Ma) is either the fossil depth of track instability, or the section with the low age gradient was formed during the rotation of the block.

The lower limit for the rotational exhumation of the Ivrea basement is confined by the apatite FT-thermochronometer, which indicates that cooling was below *c*. 100 °C and occurred around 12 Ma. The sporadic data published from the entire Ivrea complex do not reveal a trend (cf. Wagner *et al.* 1977; Hurford 1986; Hunziker *et al.* 1992). It is difficult to interpret these ages as providing kinematic evidence, because the young apatite FT data are mainly controlled by the Late Neogene exhumation of the western Alps (Fügenschuh & Schmid 2003), and the very rugged local relief also has an impact on the age pattern (see e.g. Stüve *et al.* 1994).

Summary and conclusions

Structural observations at the macro- to microscopic scale characterize the Rosarolo shear zone in the upper Valstrona as a long-term shear zone which initiated during the Early Permian magmatic underplating. It accommodated extension in the lower crust under high-temperature conditions. This sinistral sense of shear is consistent with the

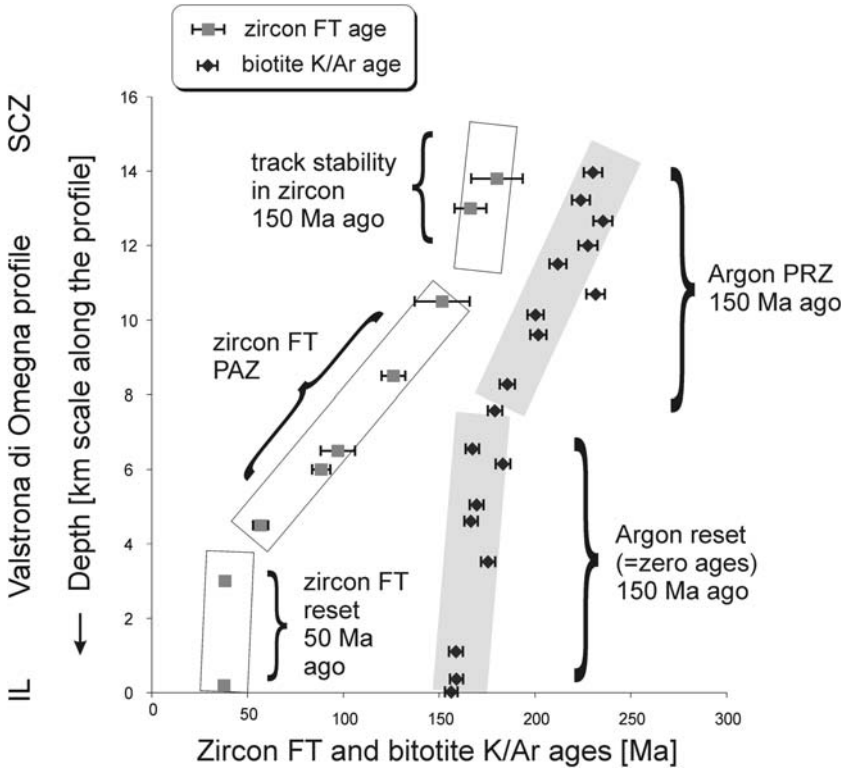

Fig. 12. Zircon FT and biotite K/Ar ages projected on an age/elevation plot. The Valstrona di Omegna profile is in the vertical position, as is hypothesized for the pre-40 Ma period. The steep intervals are the former zones of reset and a closed thermochronometer. The oblique intervals are exhumed partial retention and partial annealing zones (PRZ and PAZ respectively, for argon and FT chronometers).

gabbro-glacier growth of the Mafic Complex (see Quick *et al.* 1994). Its reactivation at different crustal levels during Mesozoic subsidence and final Eocene tilting is documented by structures indicating strain increments at different P/T conditions. Due to the late overall *c.* 90 ° tilt of this crustal section, the former extensional mylonites currently appear as a left-lateral transform shear zone. In order to confine the timing of this vertical rise, different isotopic systems along the Valstrona were analysed. They all show coherent age progression patterns related to the Late Variscan to Neo-Alpine geodynamic evolution of the Ivrea Zone's basement (Figs 12 and 13).

U–Pb monazite ages between 292 Ma and 274 Ma (Henk *et al.* 1997) are rather uniform. The younger ages in proximity to the Insubric Line, formerly the deepest part of the crust, are explained by the heat input by mafic melts leading to the complete equilibration of the U–Pb system in monazite. Recent high estimates on the closure temperature at 725 °C or even 800 °C of this isotope system point out that the monazite ages at 292 Ma at upper crustal levels of the IVZ reflect incomplete isotope reset and that the pre-Permian metamorphic peak is still an open question. Evidence for pre-Permian ages is only known from a few monazite ages in the SCZ. This contrasts with earlier interpretations based on numerical simulations on the temperature degradation with lower U–Pb closure temperatures for monazite (Henk *et al.* 1997), suggesting a complete obliteration of any pre-Permian geochronological record in the IVZ. However, considering the more recently reported SHRIMP-data by Peressini *et al.* (2007), who found out that the Mafic Complex grew from 290 (or earlier) to 288 Ma, the question arises whether the youngest monazite ages are simple cooling ages or the result of the latest events of underplating.

The age of the main metamorphic event in the SCZ is Early Palaeozoic (*c.* 450 Ma). $^{40}Ar/^{39}Ar$ hornblende data (Boriani & Villa 1997) point to a Variscan overprint at 320–350 Ma. These findings are in agreement with the oldest K–Ar biotite ages of *c.* 345 Ma in Lesa at the lakeside of Lago Maggiore. Hence, the K–Ar biotite ages for the Baveno granite at *c.* 291–284 Ma support the concept that

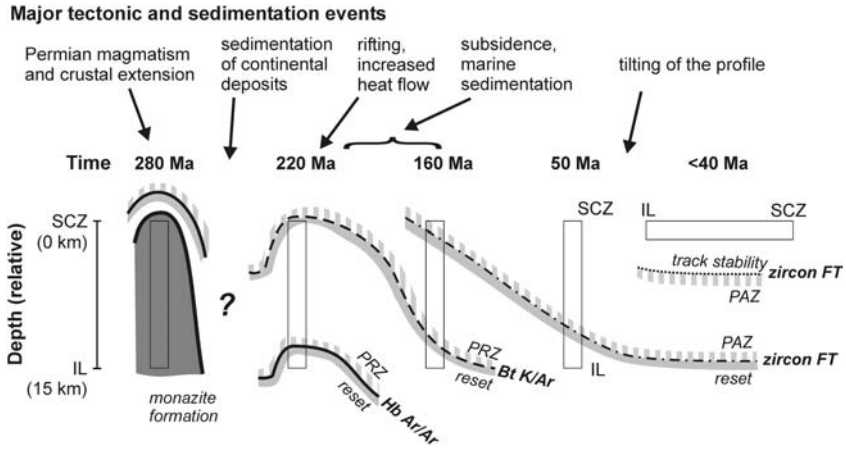

Fig. 13. Evolution of the Valstrona di Omegna profile through time (IL, Insubric Line; SCZ, Strona–Ceneri Zone). The long rectangles represent the profile, whereby it maintained a vertical position until *c*. 50 Ma, and then it was tilted to the present horizontal position at around 40 Ma ago. The curved lines express the approximate relation of the closure of the different isotope chronometers to the profile. The absolute depth of the profile cannot be determined. However, its position experienced a minor change, and the closure isotherms had a significant vertical oscillation driven by the basal heat flow and stretching of the lithosphere. PRZ, partial retention of argon; PAZ, partial annealing of fission tracks; reset, the decay products are not stable in the crystal, and the geochronometer shows zero age.

this pluton was emplaced in an already cooled basement with temperatures less than or equal to 300 °C. Its shallow emplacement level is also evident by the larger amount of miarolitic cavities.

The other applied chronometers, i.e. Ar-systematics in hornblende and biotite as well as the zircon fission-track data, document the cooling of the crust after the Permian underplating of mafic melts. Well-defined and roughly parallel age progressions of the hornblende and biotite data show a decrease from the Pogallo Line towards the Insubric Line cross-cutting the CMB Line, i.e. downwards from the middle continental crust to lower crustal levels. Carefully evaluated $^{40}Ar/^{39}Ar$ hornblende raw data yield ages from *c*. 271 Ma to *c*. 201 Ma. K–Ar biotite ages on the same distance range from *c*. 230 Ma to 156 Ma, whereas the zircon FT ages between 180 Ma to 38 Ma bracket a much broader time interval. No significant offsets of these ages are manifested, neither across the contact between the IVZ and the SCZ, as characterized by the CMB mylonites (Boriani & Giobbi 2004), the Pogallo Line, nor the Rosarolo shear zone. The mechanical juxtaposition of the IVZ against the SCZ along the CMB and/or Pogallo Lines is still under debate. Their juxtaposition exclusively during Early Mesozoic extensional shearing along the Pogallo Shear Zone is not documented in our data. It turns out that the CMB and Pogallo Lines do not disturb the post-Permian geochronology of the Ivrea Zone's basement. Missing age constraints on the displacement along the CMB Line is caused by the Late Permian thermal event that reset the monazite ages (see discussion above), or alternatively the total amount of displacement along the CMB was little or below the resolution of the applied methods. However, significant crustal attenuation between 2 and 4 km during the Early Permian to Middle Triassic has been proposed (Brodie & Rutter 1987; Henk *et al.* 1997). Three kilometres of crustal thinning some time during the Early Permian to Middle Triassic along the Pogallo Line was inferred from the cooling ages (Handy 1987). However, this is not confirmed by the $^{40}Ar/^{39}Ar$ hornblende and K–Ar biotite ages along the Valstrona, which show a roughly monotonous decrease towards the deeper part of the crust. The new data may confirm current interpretations of the Pogallo Line as a Mesozoic low-angle normal fault subsequently rotated into a steep orientation during Neo-Alpine times. The restoration of the IVZ–SCZ basement to a pre-Alpine configuration (Handy 1987; Schmid *et al.* 1987) explains the oblique low-angle normal fault. The deeper level is exposed in the Val Cannobino, whereas the upper level with a broader zone of cataclasis is exposed in the Valstrona.

Both the K–Ar biotite and the zircon FT age trends show a break-in-slope at roughly 160 Ma (Late Jurassic) after the end of the formation of Jurassic rift structures. This led to the formation of the Piedmont-Ligurian Ocean as part of the Tethys, probably during and after the sinking and stabilization of the perturbed isotherms. The intervals of gradual

change of ages, interpreted as an exhumed partial argon retention zone and/or partial stability zone of zircon fission tracks, respectively, document the progressive cooling of the crust previously (K–Ar biotite data) and subsequently (zircon fission track data) to the Jurassic extension. The upper break-in-slope of the zircon fission track ages at *c*. 50 Ma, interpreted to be formed during, or immediately after the rotation of the IVZ, is consistent with the main Neo-Alpine collision during the Eocene. No evidence was found for any individual rotational uplift of the two basement slices or that tilting already took place earlier in the evolution.

With this paper, we wish to remember our colleague Hans Ahrendt who carried out most of the mapping in the Ivrea Zone, and almost all of the K–Ar analyses together with Petra Clausen and Doris Jaeger. Special thanks go to the staff of the nuclear reactors of Oregon State University and McMaster University for their careful neutron irradiations. For help with the sampling, we would like to thank Stefan Mosch and Pedro Oyhantcabal. For very helpful comments, we are most grateful to S. Sinigoi, B. Fügenschuh, J.H. Kruhl and S. Schmid.

Appendix: Analytical methods

$^{40}Ar/^{39}Ar$ hornblende dating

Eleven hornblende separates were dated at the Geochronology Laboratory of the Geophysical Institute of the University of Alaska Fairbanks. The monitor mineral MMhb-1 (Samson & Alexander 1987) with an age of 513.9 Ma (Lanphere & Dalrymple 2000) was used to check the neutron flux and calculate the irradiation parameter (J) for all samples. The samples and standards were wrapped in aluminium foil and loaded into aluminium cans of 2.5 cm diameter and 6 cm height. All samples were irradiated in position 5c of the uranium-enriched research reactor of McMaster University in Hamilton, Ontario, Canada for 30 megawatt-hours.

Upon their return from the reactor, the samples and monitors were loaded into 2 mm-diameter holes in a copper tray that was then loaded in an ultra-high vacuum extraction line. The monitors were fused, and samples heated, using a 6-watt argon-ion laser following the techniques described in York *et al.* (1981), Layer *et al.* (1987) and Layer (2000). Argon purification was achieved using a liquid nitrogen cold trap and a SAES Zr–Al getter at 400 °C. The samples were analysed in a VG-3600 mass spectrometer. The measured argon isotopes were corrected for system blank and mass discrimination, as well as calcium, potassium and chlorine interference reactions following procedures outlined in McDougall and Harrision (1999). System blanks generally were 2×10^{-16} mol ^{40}Ar and 2×10^{-18} mol ^{36}Ar that are 10 to 50 times smaller than fraction volumes. Mass discrimination was monitored by running both calibrated air shots and a zero-age glass sample. All ages are quoted to the ± 1 sigma level and were calculated using the constants of Steiger and Jäger (1977). The integrated ages is the age given by the total gas measured and is equivalent to a potassium–argon (K–Ar) age. The spectrum provides a plateau age if three or more consecutive gas fractions represent at least 50% of the total gas release and are within two standard deviations of each other (Mean Square Weighted Deviation less than *c*. 2.5).

K–Ar dating of biotite samples

Mica separation was performed by the standard techniques such as crushing, sieving, using the Frantz magnetic separator and selection by hand. The pure micas were ground in alcohol and sieved to remove altered rims which might have suffered argon loss.

The argon isotopic composition was measured in a Pyrex glass extraction and purification line coupled to a VG 1200 C noble gas mass spectrometer operating in static mode. The amount of radiogenic ^{40}Ar was determined by the isotopic dilution method using a highly enriched ^{38}Ar spike from Schumacher, Bern (Schumacher 1975). The spike is calibrated against the biotite standard HD-B1 (Fuhrmann *et al.* 1987). The age calculations are based on the constants recommended by the IUGS quoted in Steiger & Jäger (1977).

Potassium was determined in duplicate by flame photometry using an Eppendorf Elex 63/61. The samples were dissolved in a mixture of Hf and HNO_3 according to the technique of Heinrichs & Herrmann (1990). CsCl and LiCl were added as an ionization buffer and internal standard, respectively. The analytical error for the K–Ar age calculations has a 95% confidence level of 2σ. The procedural details for argon and potassium analyses at the laboratory in Göttingen are given in Wemmer (1991).

Zircon fission-track dating

The zircon crystals were collected by using a heavy liquid and magnetic separation, and then the crystals were embedded in PFA Teflon. To reveal the spontaneous tracks, the eutectic melt of NaOH-KOH was used at the temperature of 225 °C (Gleadow *et al.* 1976). The etching time varied from 23–54 hours. Neutron irradiations were made at the research reactor of Oregon Sate University. The external detector method was used (Gleadow 1981); after irradiation, the induced fission tracks in the mica detectors were revealed by etching in 40% HF acid for 30 min. Track counts were made with a Zeiss-Axioskop microscope (magnification of 1000) and a computer-controlled stage system (Dumitru 1993). The FT ages were determined by the ZETA method (Hurford & Green 1983) using age standards listed in Hurford (1998). The error was calculated using the classical procedure, i.e. by Poisson dispersion (Green 1981). Calculations and plots were made with the TRACKKEY program (Dunkl 2002).

References

AHRENDT, H., CLAUSEN, P. & VOLLBRECHT, A. 1990. Long-term shear zones in lower crustal rocks: an example from the Ivrea zone (Italian Alps). *Symposium Deformation Processes and the Structure of the Lithosphere*, Potsdam, May 3rd–10th, abstracts: p. 1.

BERCKHEMER, H. 1969. Direct evidence for the composition of the lower crust and Moho. *Tectonophysics*, **8**, 97–105.

BERTOLANI, M. 1969. La Petrografia delle Valle Strona (Alpi Occidentale Italiane). *Schweizerische Mineralogische und Petrographische Mitteilunngen*, **49**, 314–328.

BERTOTTI, G. 1991. Early Mesozoic extension and Alpine shortening in the western southern Alps: the geology of the area between Lugano and Menaggio (Lombardy, Northern Italy). *Memorie di Scienze Geologiche Padova*, **43**, 17–123.

BORIANI, A. & GIOBBI, E. 2004. Does the basement of western southern Alps display a tilted section through the continental crust? A review and discussion. *Periodico di Mineralogia*, **73**, 5–22.

BORIANI, A. & VILLA, I. 1997. Geochronology of regional metamorphism in the Ivrea–Verbano Zone and Serie dei Laghi, Italian Alps. *Schweizerische Mineralogische und Petrographische Mitteilungen*, **77**, 381–402.

BORIANI, A., ORIGONI GIOBBI, E., BORGHI, A. & CAIRONI, V. 1990. The evolution of the 'Serie dei Laghi' (Strona-Ceneri and Schisti dei Laghi): The upper component of the Ivrea–Verbano crustal section; southern Alps, north Italy and Ticino, Switzerland. *Tectonophysics*, **182**, 103–118.

BRODIE, K. & RUTTER, E. 1987. Deep crustal extensional faulting in the Ivrea zone of Northern Italy. *Tectonophysics*, **140**, 193–212.

BRODIE, K., REX, D. & RUTTER, E. 1989. On the age of deep crustal extensional faulting in the Ivrea Zone, northern Italy. *In*: COWARD, M. P., DIETTRICH, D. & PARK, R. G. (eds) *Alpine Tectonics*. Geological Society Special Publication, **45**, 203–210.

BRODIE, K., RUTTER, E. & EVANS, P. J. 1992. On the structure of the Ivrea–Verbano Zone (N. Italy) and its implication for present day lower continental crust geometry. *Terra Nova*, **4**, 34–40.

CLAUSEN, P. 1990. *Systematische K/Ar-Altersbestimmungen an Biotite in einem Querprofil durch die Ivrea-Verbano Zone (Val Strona di Omegna, Provinz Novara, Norditalien)*. Unpublished Diploma thesis, University Göttingen, 1–40.

COPELAND, P., PARRISH, R. R. & HARRISON, T. M. 1988. Identification of inherited radiogenic Pb in monazite and its implications for U–Pb systematics. *Nature*, **333**, 760–763.

DAHL, P. S. 1996. The effects of composition on retentivity of Ar and O in hornblende and related amphiboles: a field-tested empirical model. *Geochemica et Cosmochimica Acta*, **60**, 3687–3700.

DORNBUSCH, H.-J. & SKROTZKI, W. 2001. Microstructure and texture formation in a high-temperature shear-zone—with emphasis on amphibole. *In*: SIEGESMUND, S. (ed.) *Festschrift Klaus Weber*. Zeitschrift der Deutschen Geologischen Gesellschaft, **152**, 503–526.

DUMITRU, T. 1993. A new computer-automated microscope stage system for fission-track analysis. *Nuclear Tracks and Radiation Measurement*, **21**, 575–580.

DUNKL, I. 2002. TRACKKEY: a Windows program for calculation and graphical presentation of fission track data. *Computers & Geosciences*, **28**, 3–12.

FOUNTAIN, D. M. 1976. The Ivrea–Verbano and Strona-Ceneri zones, northern Italy: a cross section of the continental crust—new evidence from seismic velocities. *Tectonophysics*, **33**, 145–166.

FOUNTAIN, D. M. 1986. Implication of deep crustal evolution for seismic reflection seismology. *In*: BARAZANGI, M. & BROWN, L. (eds) *Reflection Seismology: The Continental Crust.* American Geophysical Union, Geodynamic Series, **14**, 1–7.

FOUNTAIN, D. M. 1989. Growth and modification of lower continental crust in extended terrains: the role of extension and magmatic underplating. *In*: MEREU, R. F., MUELLER, S. & FOUNTAIN, D. M. (eds) *Lower Crust Properties and Processes.* American Geophysical Union Monographs, **51**, 287–299.

FOUNTAIN, D. M. & SALISBURY, M. H. 1981. Exposed cross section through the continental crust: Implication for crustal structure, petrology and evolution. *Earth and Planetary Science Letters*, **5**, 263–277.

FÜGENSCHUH, B. & SCHMID, S. M. 2003. Late stage of deformation and exhumation of an orogen constrained by fission-track data: A case study of the Western Alps. *The Geological Society of America Bulletin*, **115**, 1425–1440.

FUHRMANN, U., LIPPOLT, H. J. & HESS, J. C. (1987) Examination of some proposed K–Ar standards: $^{40}Ar/^{39}Ar$ analyses and conventional K–Ar-Data. *Chemical Geology (Isotopic Geoscience Section)*, **66**, 41–51.

GARUTTI, G., RIVALENTI, G., ROSSI, A. & SINIGOI, S. 1978/1979. Mineral equilibria as geotectonic indicators in the ultramafics and related rocks of the Ivrea-Verbano Basic Complex (Italian Western Alps) Pyroxenes and Olivine. *Memorie di Scienze Geologiche*, **33**, 147–160.

GLEADOW, A. J. W. 1981. Fission-track dating methods: what are the real alternatives? *Nuclear Tracks*, **5**, 3–14.

GLEADOW, A. J. W., HURFORD, A. J. & QUAIFE, R. D. 1976. Fission track dating of zircon: improved etching techniques. *Earth and Planetary Research Letters*, **33**, 273–276.

GREEN, P. F. 1981. A new look at statistics in fission track dating. *Nuclear Tracks*, **5**, 77–86.

HANDY, M. R. 1987. The structure, age and kinematics of the Pogallo fault zone, southern Alps, northwestern Italy. *Eclogae Geologicae Helvetiae*, **80**, 593–632.

HANDY, M. R. & ZINGG, A. 1991. The tectonic and rheological evolution of an attenuated cross section of the continental crust: Ivrea crustal section, southern Alps, northwestern Italy and southern Switzerland. *Geological Society American Bulletin*, **103**, 236–253.

HANDY, M. R., FRANZ, L., HELLER, F., JANOTT, B. & ZURBRIGGEN, R. 1999. Multistage accretion and exhumation of the continental crust (Ivrea crustal

section, Italy and Switzerland). *Tectonics*, **18**, 1154–1177.

HARTMANN, G. & WEDEPOHL, K. H. 1993. The composition of peridotite tectonites from the Ivrea Complex, northern Italy: residues from melt extraction. *Geochemica et Cosmochimica Acta*, **57**, 1761–1782.

HEINRICHS, H. & HERRMANN, A. G. 1990. *Praktikum der Analytischen Geochemie*. Springer Verlag.

HENK, A., FRANZ, L., TEUFEL, S. & ONCKEN, O. 1997. Magmatic underplating, extension and crustal reequilibration: insight from a cross section through the Ivrea-Verbano Zone and Serie del Laghi. N.W. Italy. *Journal of Geology*, **105**, 367–377.

HODGES, K. V. & FOUNTAIN, D. M. 1984. Pogallo Line, South Alps: an intermediate crustal level, low-angle normal fault. *Geology*, **12**, 151–155.

HUNZIKER, J. & ZINGG, A. 1980. Lower Paleozoic amphibolite to granulite facies metamorphism in the Ivrea Zone (southern Alps, northern Italy). *Schweizerische Mineralogische und Petrographische Mitteilungen*, **60**, 181–213.

HUNZIKER, J., DESMONS, J. & HURFORD, A. J. 1992. Thirty-two years of geochronological work in the Central and Western Alps: a review on seven maps. *Memoires de Geologie Lausanne*, **13**, 1–59.

HURFORD, A. J. 1986. Cooling and uplift patterns in the Lepontine Alps South Central Switzerland and an age of vertical movement on the Insubric fault line. *Contributions to Mineralogy and Petrology*, **93**, 413–427.

HURFORD, A. J. 1998. Zeta: the ultimate solution to fission-track analysis calibration or just an interim measure? *In*: VAN DEN HAUTE, P. & DE CORTE, F. (eds) *Advances in Fission-Track Geochronology*. Kluwer Academic Publishers, 19–32.

HURFORD, A. J. & GREEN, P. F. 1983. The zeta age calibration of fission-track dating. *Chemical Geology* (*Isotopic Geoscience Section*), **41**, 285–312.

KAMP, P. J. J., GREEN, P. F. & WHITE, S. H. 1989. Fission track analysis reveals character of collisional tectonics in New Zealand. *Tectonics*, **8**, 169–195.

KAMBER, B. S., KRAMERS, J. D., NAPIER, R., CLIFF, R. A. & ROLLINSON, H. R. 1995. The Triangle Shear Zone, Zimbabwe, revisited: new data document an important event at 2.0 Ga in the Limpopo Belt. *Precambrian Research*, **70**, 191–213.

KAMBER, B. S., FREI, R. & GIBBS, A. J. 1998. Pitfalls and new approaches in granulite chronometry. An example from the Limpopo Belt. *Precambrian Research*, **91**, 269–285.

KÖPPEL, V. 1974. Isotopic U-Pb ages of monazite and zircons from the crust-mantle transition and adjacent units of the Ivrea and Strona-Ceneri Zones (southern Alps). *Schweizerische Mineralogische und Petrographische Mitteilungen*, **51**, 385–409.

KÖPPEL, V. & GRÜNFELDER, M. 1978/1979. Monazite and zircon U–Pb ages from the Ivrea and Ceneri Zones (southern Alps, Italy). *Memorie di Scienze Geologiche*, **33**, 55–70.

LANPHERE, M. A. & DALRYMPLE, G. B. 2000. First-principles calibration of ^{38}Ar tracers: Implications for the ages of ^{40}Ar/^{39}Ar fluence monitors. *U.S. Geological Survey Professional Paper*, **1621**, 10.

LANZIROTTI, A. & HANSON, G. N. 1996. Geochronology and geochemistry of multiple generations of monazite from the Wepawaug Schist, Connecticut, USA: implication for monazite stability in metamorphic rocks. *Contributions to Mineralogy and Petrology*, **125**, 332–340.

LAYER, P. W. 2000. Argon-40/Argon-39 age of the El'gygytgyn impact event, Chukotka, Russia. *Meteoritics and Planetary Science*, **35**, 591–599.

LAYER, P. W., HALL, C. M. & YORK, D. 1987. The derivation of ^{40}Ar/^{39}Ar age spectra of single grains of hornblende and biotite by laser step heating. *Geophysical Research Letters*, **14**, 757–760.

LOGAN, J. M., FRIEDMAN, M., HIGGS, N. G., DENGO, C. & SHIMAMOTO, T. 1979. Laboratory studies of simulated gouge and their application to studies of natural fault zones. *In*: Proc. Conf. VIII, Analysis of actual fault zones in bedrock. *U.S. Geological Survey Open File Rep.*, **79**, 305–343.

MCDOUGALL, I. & HARRISON, T. M. 1999. *Geochronology and thermochronology by the ^{40}Ar/^{39}Ar Method.* (2nd edn), Oxford University Press, New York.

MEHNERT, K. 1975. The Ivrea zone, a model of the deep crust. *Neues Jahrbuch Mineralogie Abhandlungen*, **125**, 156–199.

METZGER, K., RAWNSLEY, C. M., BOHLEN, S. R. & HANSON, G. N. 1991. U–Pb garnet, sphene, monazite and rutile ages; implication for the duration of high-grade metamorphism and cooling histories, Adirondack Mts., New York. *Journal of Geology*, **99**, 415–428.

MULCH, A., ROSENAU, M., DÖRR, W. & HANDY, M. R. 2002. The age and structure of dikes along the tectonic contact of the Ivrea–Verbano and Strona-Ceneri Zones (southern Alps, Northern Italy, Switzerland). *Schweizerische Mineralogische und Petrographische Mitteilungen*, **82**, 55–76.

NOVARESE, V. 1929. La Zona del Canavese e le formazioni adiacenti. *Memorie Descrittive Della Carta Geologia d'Italia*, **22**, 65–212.

PARRISH, R. R. 1990. U-Pb dating of monazite and its application to geological problems. *Canadian Journal of Earth Sciences*, **27**, 1431–1450.

PIN, C. 1986. Datation U-Pb sur zircons a 285 M.a. du complex gabbro-dioritique du Val Sesia-Val Mastallone et age tardi-hercyien du metamorphisme granitique de la zone Ivrea–Verbano (Italie), *Comptes Rendu de L'Academie des Sciences, Paris*, **303**, 827–830.

PERESSINI, G., QUICK, J. E., SINIGOI, S., HOFFMANN, A. W. & FANNING, M. 2007. Duration of a large mafic intrusion and heat transfer in the lower crust: a SHRIMP U–Pb zircon study in the Ivrea–Verbano Zone (Western Alps, Italy). *Journal of Petrology*, **50**, 1–34.

PURDY, J. W. & JAEGER, E. 1976. K-Ar ages on rock-forming minerals from the central Alps. *Memorie degli Istituti di Geologia e Mineralogia dell'Universita di Padova*, **30**, 1–321.

QUICK, J., SINIGOI, S. & MAYER, A. 1994. Emplacement of mantle peridotite in the lower continental crust, Ivrea Verbano Zone, Northwestern Italy. *Journal of Geophysical Research*, **99**, 21559–21573.

RABBEL, W., SIEGESMUND, S., WEISS, T., POHL, M. & BOHLEN, T. 1998. Shear wave anisotropy of the laminated lower crust beneath Urach (SW Germany) - a comparison with xenoliths and with exposed lower crustal sections. *Tectonophysics*, **298**, 337–356.

RIGALETTI, A. R., HEBEDA, E. H., SIGNER, P. & WIELER, R. 1994. Uranium–xenon chronology: precise determination of λ_{sf} $^{136}Y_{sf}$ for spontaneous fission of ^{238}U. *Earth and Planetary Science Letters*, **128**, 653–670.

RIVALENTI, G., GARUTI, G. & ROSSI, A. 1975. The origin of the Ivrea-Verbano basic formation (western Italian Alps): Whole rock geochemistry. *Bollettino della Società Geologica Italiana*, **94**, 1149–1186.

RIVALENTI, G., GARUTI, G., ROSSI, A., SIENA, F. & SINIGOI, S. 1981. Existence of different peridotite types and of a layered igneous complex in the Ivrea Zone of the western Alps. *Journal of Petrology*, **22**, 127–153.

RUTTER, E., BRODIE, K. & EVANS, P. 1993. Structural geometry, lower crustal magmatic underplating and lithospheric stretching in the Ivrea–Verbano Zone, N. Italy. *Journal of Structural Geology*, **15**, 647–552.

RUTTER, E., BRODIE, K., JAMES, T. & BURLINI, L. 2007. Large-scale folding in the upper part of the Ivrea–Verbano zone, NW Italy. *Journal of Structural Geology*, **29**, 1–17.

SAMSON, S. D. & ALEXANDER, E. C. 1987. Calibration of the interlaboratory $^{40}Ar/^{39}Ar$ dating standard, MMhb1. *Chemical Geology*, **66**, 27–34.

SAWKA, W. N., BANFIELD, J. F. & CHAPELL, B. W. 1986. A weathering-related origin of widespread monazite in S-type granites. *Geochemica et Cosmochimica Acta*, **50**, 171–175.

SCHMID, R. 1978/1979. Are the metapelites in the Ivrea Zone restites? *Memorie di Scienze Geologiche*, **33**, 67–69.

SCHMID, S. M. 1993. Ivrea zone and adjacent southern Alpine basement. *In*: VON RAUMER, J. F. & NEUBAUER, F. (eds) *Pre-Mesozoic Geology in the Alps*. Springer Verlag, New York, 567–583.

SCHMID, S. M., ZINGG, A. & HANDY, M. R. 1987. The kinematics and movements along the Insubric Line and the emplacement of the Ivrea Zone. *Tectonophysics*, **135**, 47–66.

SCHUMACHER, E. 1975. Herstellung von 99,9997% ^{38}Ar für die $^{40}K/^{40}Ar$ Geochronologie. *Geochronometria Chimia*, **24**, 441–442.

SEYDOUX-GUILLAUME, A.-M, 2001. Experimental determination of the incorporation of Th into orthophosphates and the resetting of geochronological systems of monazite, TU Berlin.

SHERVAIS, J. 1978/1979. Ultramafic and mafic layers in the Alpine-type Lherzolite massif at Balmuccia, N.W. Italy. *Memorie di Scienze Geologiche*, **33**, 135–145.

SILLS, J. D. 1984. Granulite facies metamorphism in the Ivrae zone, NW Italy. *Schweizerische Mineralogische und Petrographische Mitteilungen*, **64**, 169–191.

SILLS, J. D. & TARNEY, J. 1984. Petrogenesis and tectonic significance of amphibolites interlayered with metasedimentary gneisses in the Ivrea zone, S. Alps, N. Italy. *Tectonophysics*, **107**, 187–206.

SMITH, H. A. & BARREIRO, B. 1990. Monazite U-Pb dating of staurolite-grade metamorphism in pelitic schists. *Contributions to Mineralogy and Petrology*, **105**, 602–615.

SNOKE, A. W., KALAKAY, T. J., QUICK, J. E. & SINIGOI, S. 1999. Development of a deep crustal shear zone in response to tectonic intrusion of mantle magma into the lower crust, Ivrea-Verbano zone, Italy. *Earth and Planetary Science Letters*, **166**, 31–45.

STÄMPFLI, G. M., BOREL, G., MARCHANT, R. & MOSAR, J. 2002. Western Alps geological constraints on western Tethyan reconstructions. *Journal Virtual Explorer*, **8**, 77–106.

STEIGER, R. H. & JAEGER, E. 1977. Subcommission on geochronology: Convention on the use of decay constants in geo-and cosmochronology. *Earth and Planetary Science Letters*, **36**, 359–362.

TEUFEL, S. & SCHÄRER, U. 1989. Unravelling the age of high-grade metamorphism of the Ivrea Zone: A monazite single-grain and small fraction study. *Terra Abstract*, **1**, 350.

VAVRA, G., GEBAUER, D., SCHMID, R. & COMPSTON, W. 1996. Multiple zircon growth and recrystallisation during polyphase late Carboniferous to Triassic metamorphism in granulites of the Ivrea Zone (southern Alps): An ion microprobe (SHRIMP) study. *Contributions to Mineralogy and Petrology*, **122**, 337–358.

VILLA, I. 1998. Isotopic closure. *Terra Nova*, **10**, 42–47.

VILLA, I., GROBERTY, B. H., KELLEY, S. P., TRIGLIA, R. & WIELER, R. 1996. Assessing Ar transport paths and mechanisms in the McClure Mountains hornblende. *Contributions to Mineralogy and Petrology*, **126**, 67–80.

VOSHAGE, H., SINIGOI, S., MAZZUCHELLI, M. G., RIVALENTI, G. & HOFMANN, A. W. 1988. Isotopic constraints on the origin of ultramafic and mafic dikes in the Balmuccia peridotite (Ivrea Zone). *Contributions to Mineralogy and Petrology*, **100**, 261–267.

VOSHAGE, H., HOFMANN, A. W., MAZUCHELLI, G., RIVALENTI, G., SINIGOI, S., RACZEK, I. & DEMARCHI, G. 1990. Isotopic evidence from the Ivrea Zone for a hybrid lower crust formed by magmatic underplating. *Nature*, **347**, 731–736.

WAGNER, G. A., REIMER, G. M. & JÄGER, E. 1977. Cooling ages derived by apatite fission-track, mica Rb-Sr and K-Ar dating: the uplift and cooling history of the Central Alps. *Memorie Instituti di Geologia di Padova*, **XXX**, 1–28.

WEISS, T., SIEGESMUND, S., RABBEL, W., BOHLEN, T. & POHL, M. 1999. Physical properties of the Lower continental crust: an anisotropic perspective. *Pure and Applied Geophysics*, **156**, 97–122.

WEMMER, K. 1991. K/Ar-Altersdatierungsmöglichkeiten für retrograde Deformationsprozesse im spröden und duktilen Bereich–Beispiele aus der KTB-Vorbohrung (Oberpfalz) und dem Bereich der Insubrischen Linie (N-Italien). *Göttinger Arbeiten Geologie & Paläontologie*, **51**, 1–61.

YORK, D., HALL, C. M., YALANSE, Y., HANES, J. A. & KENYON, W. J. 1981. $^{40}Ar/^{39}Ar$ dating of terrestrial minerals with a continuous laser. *Geophysical Research Letters*, **8**, 1136–1138.

ZINGG, A. 1983. The Ivrea and Strona-Ceneri Zones (southern Alps, Ticino and N-Italy): A review. *Schweizerische Mineralogische und Petrographische Mitteilungen*, **77**, 361–380.

ZINGG, A., HANDY, M. R., HUNZIKER, J. & SCHMID, S. M. 1990. Tectonometamorphic history of the Ivrea Zone and its relationship to the crustal evolution of the southern Alps. *Tectonophysics*, **182**, 169–192.